Petroleum Resource Potential of the Tofino Basin.

Report prepared for
University of Victoria (UVic) –

Ministry of Energy, Mines and Petroleum Resources (MEMPR)

Partnership Program

Dr. Torge Schuemann
Dr. Michael Whiticar
Dr. Kristin Rohr

School of Earth and Ocean Sciences
University of Victoria

Executive summary

This report provides a scientific assessment of the conventional petroleum resource potential of the Tofino Basin area derived from Tertiary sources. The Tofino Basin is a frontier exploration area with limited information available. Lateral continuity of drilled lithologies, composition of sediments in the deepest and un-drilled rift section, and history of fault permeability are significant unknowns. Burial for most parts of the basin is insufficient for petroleum formation with the exception of one deep trench approximately 20km offshore. Although the oldest strata expected in this trench is of Oligocene/Miocene age most of the infill is much younger due to an increase in sedimentation rate during the upper Neogene and Quaternary. This limits petroleum generation to the deepest buried source rocks within this trench.

Petroleum System models (PSM) of Tertiary sourced petroleum systems along seismic reflection line 85-01 were used to study thermal maturation and hydrocarbon migration through time. The models are based on interpretation of seismic reflection data with three nearby wells providing lithologic information and calibration. Source rocks were modeled as being distributed over a depth range from 2500-6000m within the trench. Depending on the assumed heat flow they are envisaged to predominantly generate gas over the last 8 or 15 Ma, increasing significantly when source rocks were buried at a higher rate due to increased sedimentation during the upper Neogene until today. Hydrocarbon accumulations in Tertiary strata are predicted to occur in stratigraphic traps as well as stacked along faults and in anticline structures, depending on permeability of faults and how high they reach into younger strata. Most of the predicted accumulations lie below the zone of probable recent biodegradation but some might have experienced biodegradation in the past.

The overall petroleum potential of the Tofino Basin appears to be limited according to our model results and a clear distinction between more prospective areas like anticlines overlying the deep trench and it’s western and eastern flanks and less prospective areas further offshore is possible based on our findings.

Table of contents

List of figures

1. Technical summary

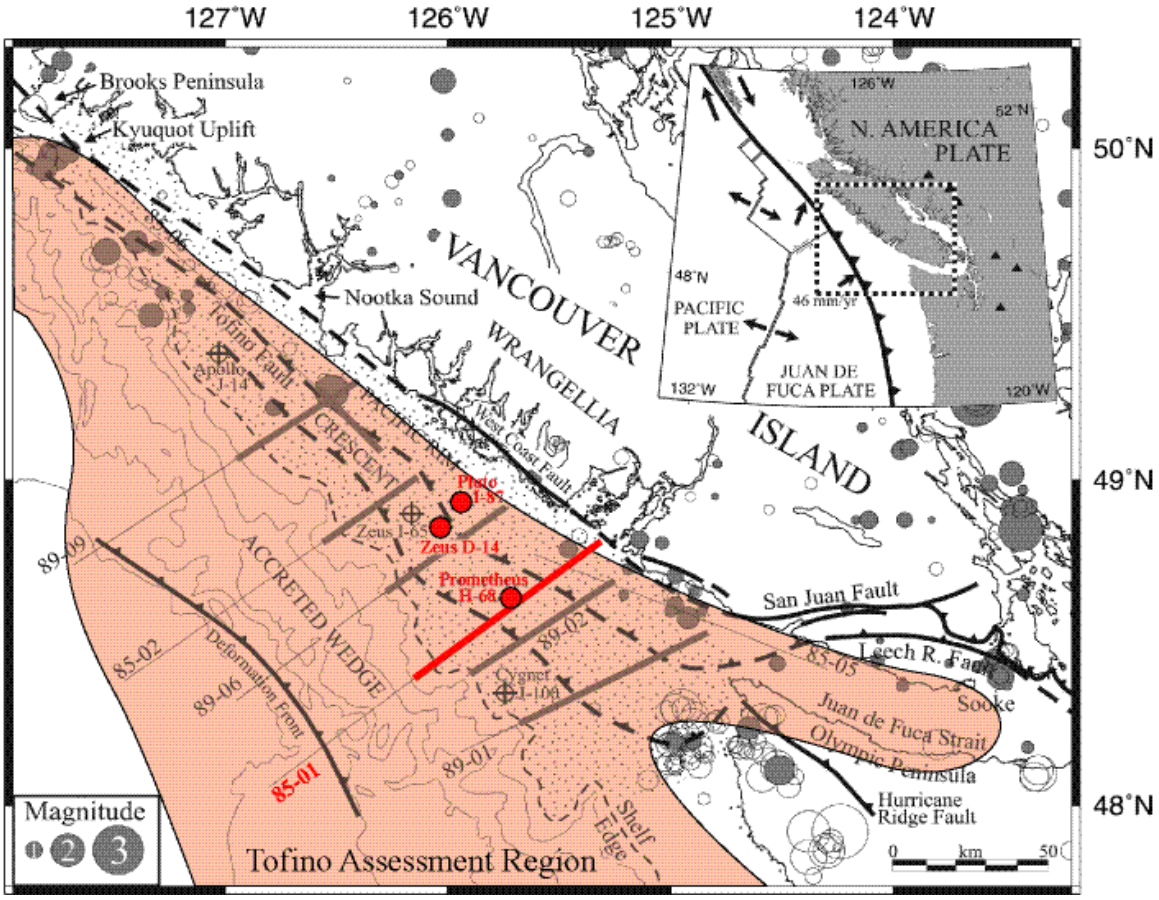

Figure 1. Map of Tofino Basin with location of seismic line 85-01 chosen for the 2D petroleum systems modeling presented in this study. Wells used for calibration are marked in red.

The Tofino Basin is a frontier exploration area with only limited information available. Along seismic reflection line 85-01, spanning the central basin from southwest to northeast Petroleum System models (PSM) of Tertiary sourced petroleum systems were studied. This enabled us to predict how thermal maturation combined with hydrocarbon migration might result in multiple accumulations of gas derived from Tertiary sources.

1.1 Input

GSC seismic reflection line 85-01 was chosen for 2D petroleum systems modeling to address hydrocarbon potential of the Tofiono Basin as it covers the central Tofino Basin and is tied directly to the Prometheus H-68 well. Lateral projection from the Pluto I-87 and the Zeus D-14 wells enables further calibration of our models. Time sections were converted to depth based on velocity profiles constructed from check shot surveys at the wells (see section 3.1).
First order stratigraphic interpretation of the Tertiary using marker horizons based on ties to the Prometheus, Pluto, and Zeus wells lead to the interpretation of 16 horizons (Figure 2 and Figure 4). For the petroleum systems modeling, additional horizons had to be added to further refine the stratigraphy

into 42 units. Layer splitting algorithms provided by the software (IES PetroMod 10.1) were used to determine their geometry, guided by reflection seismic data, where possible (see Figure 4 and section 3.1). Sensitivity to migration along/across faults was one of the scenarios tested and faults were represented in the models as either open or closed to migration or not affecting migration at all. Lateral homogeneous lithology has been assumed with lithologies derived from the Prometheus, Pluto, and Zeus wells preserving the general character of sandstones interbedded with siltstones although necessarily some layers were lumped together due to resolution constraints while building the model. Source rocks are known to occur in the Tertiary with kerogen being mainly gas prone terrestrial (type III). Standard kinetics according to Burnham (1989) were used to describe the maturation process. Information about reservoir and seal rock quality is sparse, but the general interbedded character is likely to allow for multiple trapping scenarios.

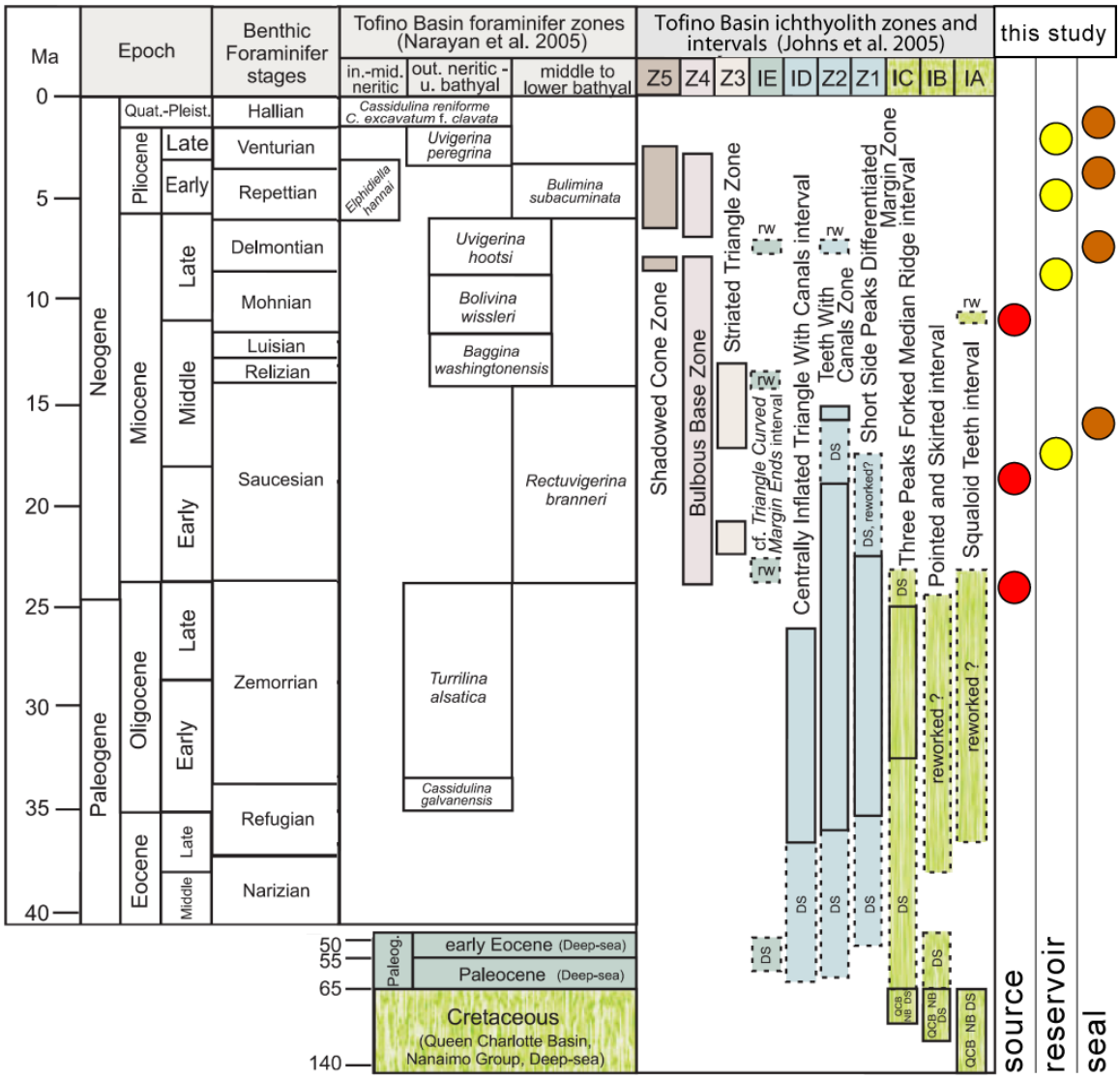

Figure 2. Modified stratigraphic chart from Johns et al (2005), showing the main stratigraphic units used to define the 2D PSM. Prominent source-, reservoir-, and seal-rock units are marked.

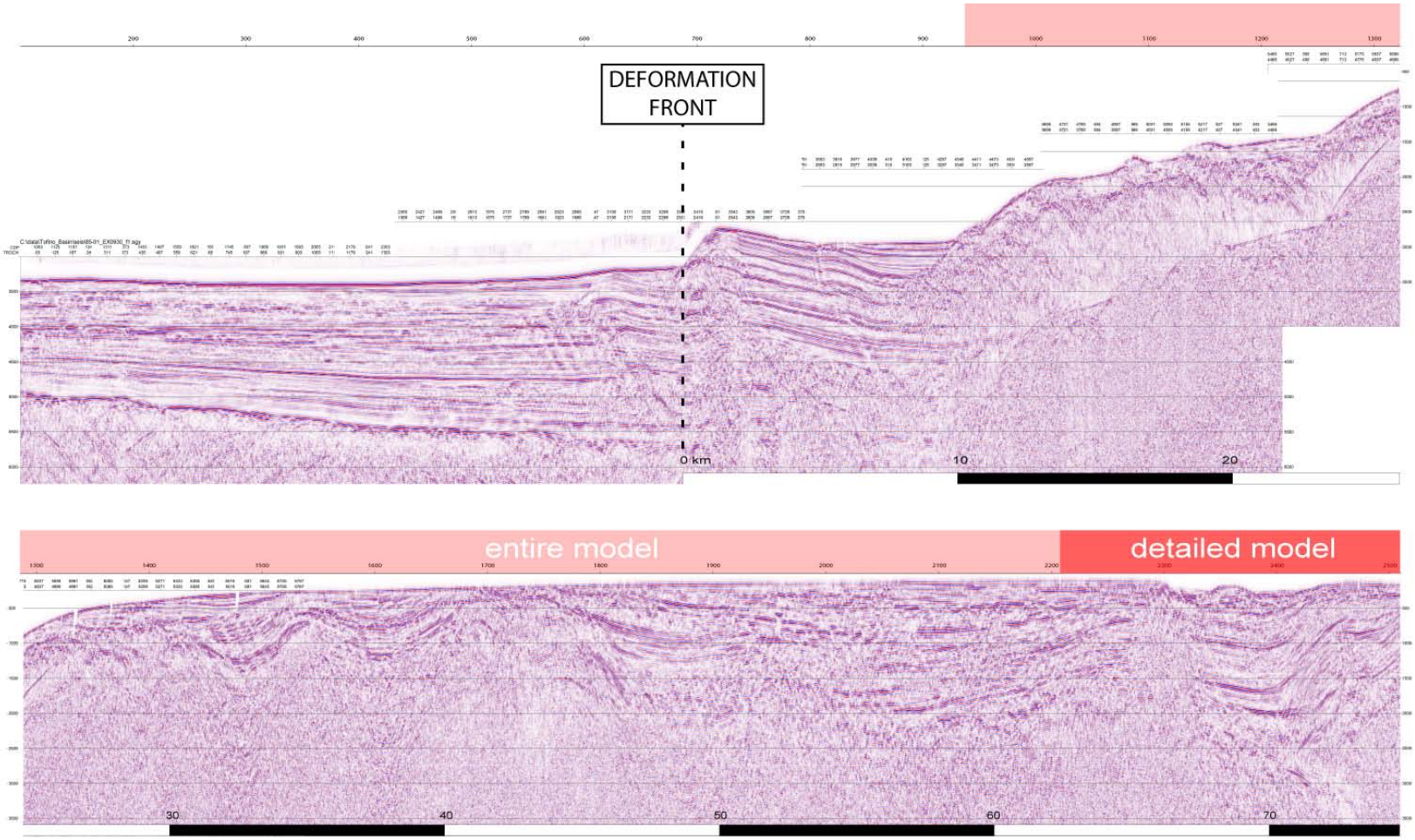

Figure 3. Reflection seismic data 85-01 with deformation front and extend of PSMs marked.

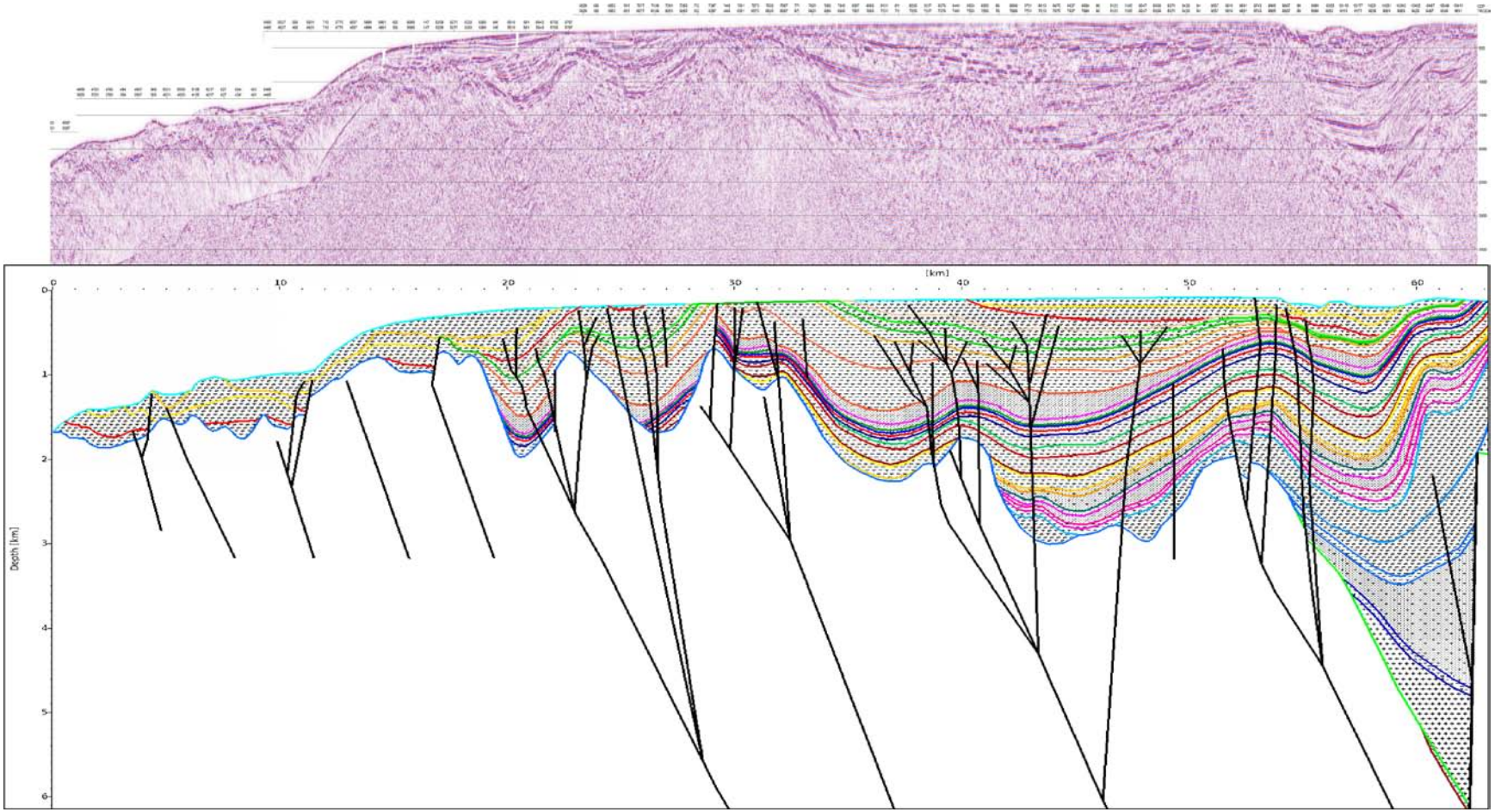

Figure 4. Reflection seismic image of the modelled part of GSC line 85-01 (above) with model interpretation (below). Note: Reflection seismic image is presented in time domain, whereas model shows interpretation converted to depth (see section 3.1).

1.2 Methods

Models tested sensitivity to different heat flow scenarios and to migration along/accross fault planes. Calibration data are sparse, with the one well (Prometheus H-68) directly positioned on the 2D model not having drilled the deepest and most mature section. Calibration data (vitrinite reflectance derived from from T_{max} temperatures) from the nearby Pluto I-87 well could however be used after projection onto the model plane and provides high quality calibration (Figure 5).
With stratigraphy and burial history derived from well ties, the heat flow history is the key remaining parameter to achieve calibration to maturation data. Best calibration to the data in the Pluto I-87 well was achieved using the 70 mW/m^2 scenario (Figure 5). However, to test for possible variation four different scenarios were investigated; three lateral and time constant ones with a heat flow of 60, 70, and 80 mW/m^2, respectively.

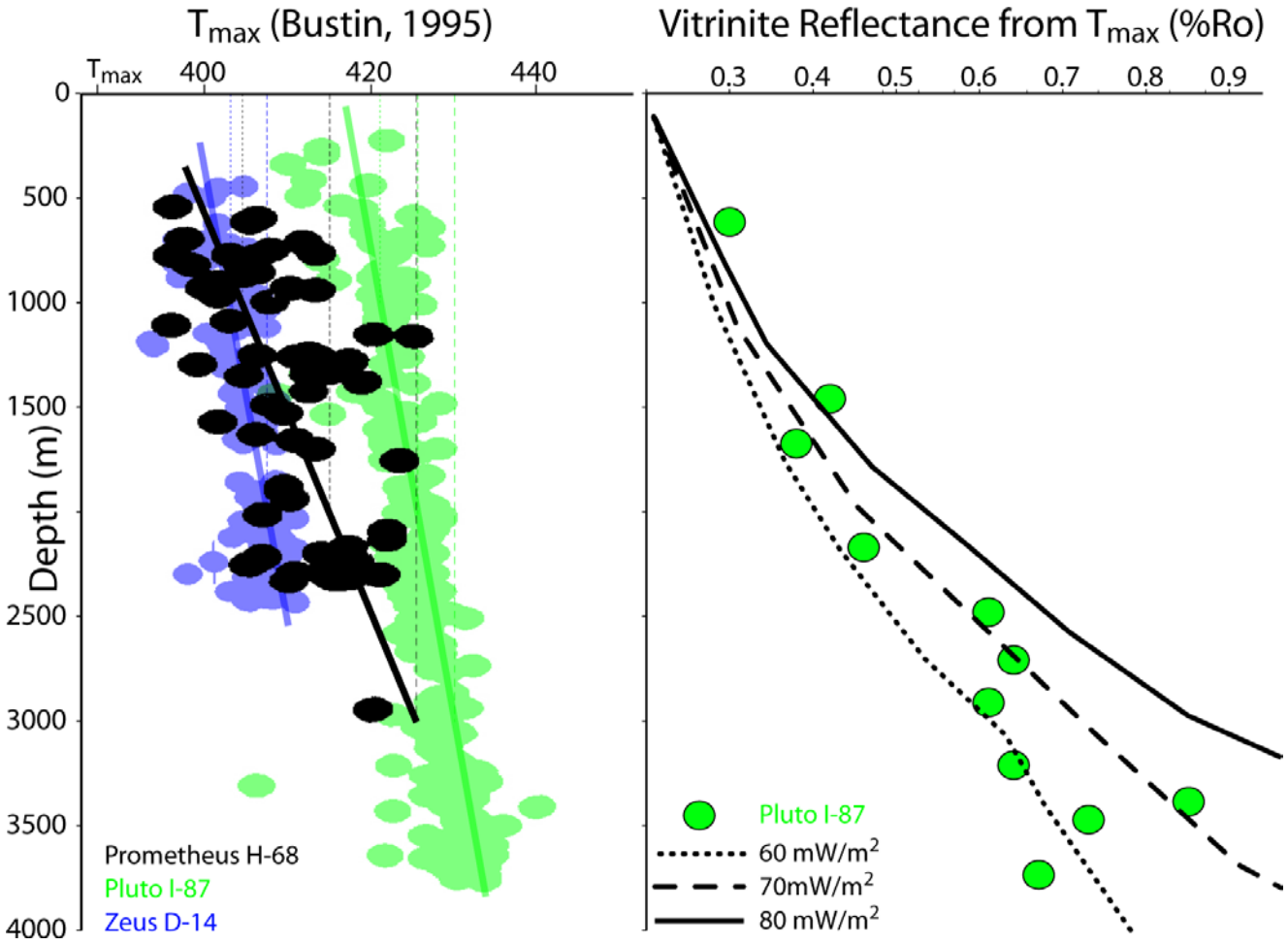

Figure 5. Calibration of 2D petroleum systems model along Line 85-01 using vitrinite reflectance derived from T_{max} temperatures (left), as reported by Bustin (1995). Only the Pluto I-87 well was drilled deep enough to record sufficiently high T_{max} temperatures to be converted into equivalent vitrinite reflectance values assuming a type III kerogen according to (Dewing and Sanei, 2008). The right panel shows calibrations achieved for a location over the deepest part of the trench. Best calibration is given for an assumed heat flow of 70mW/m^2 with 60mW/m^2 used as a lower and 80mW/m^2 as a higher end member for our sensitivity analysis.

1.3 Results

Testing for different heat flows showed differences in timing of hydrocarbon generation and expulsion. Although the onset was offset by 7Ma (15Ma @ 80mW/m^2, 8Ma @ 60mW/m^2) expulsion in all models tended to be gradual due to the varying burial of the source rocks. Comparison of the tested heat flow scenarios investigated in this study shows that varying assumptions for palaeo heat flow do not significantly affect location but size and type of hydrocarbon accumulations predicted.
Fault distribution and hydrocarbon migration along/across faults is one of the most significant factors affecting the number, size, and nature of predicted accumulations. In all but the scenarios in which faults acted sealing a substantial amount of hydrocarbon is predicted to be lost to the seafloor.

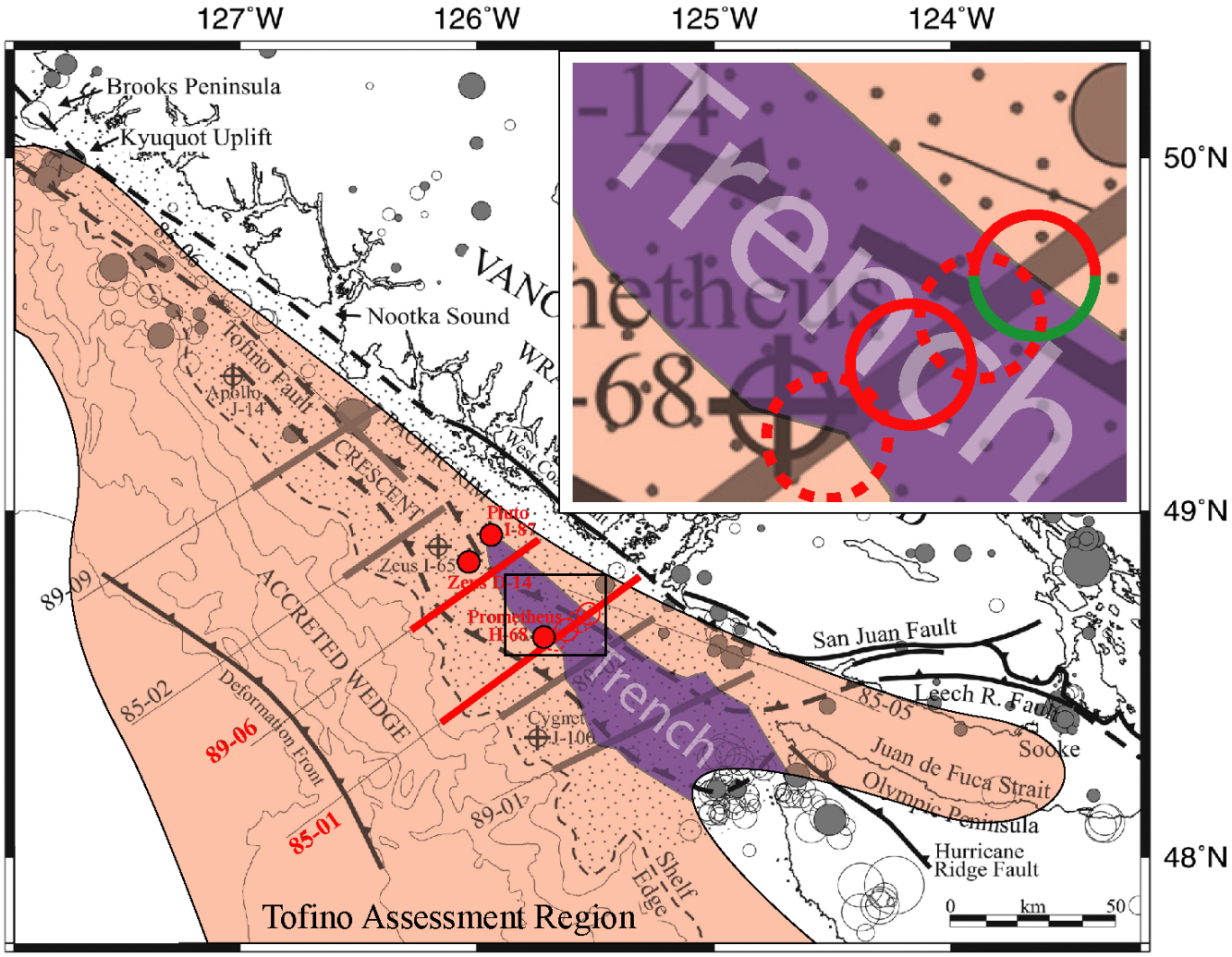

Figure 6. Bathymetry map of the Tofino Assessment Region with the sedimentary trench as interpreted based on gravity data from Dehler at al. (1992). As a first order approximation the extend of the trench equals the extend of the hydrocarbon kitchen but better mapping based on additional seismic reflection data is needed to more accurately outline its extend. Zones of predicted accumulations along the 2D transect presented in this study are shown in inset (green: oil, red: gas). Predicted accumulations in a central anticline structure and towards the southwest margin of the trench are often shallow and might be affected by recent biodegradation (dashed circles).

Figure 6 shows areas in which accumulations derived from Tertiary sources are expected to occur. Based on our assumptions most predicted accumulations are restricted to the flanks of deep trench evident in the gravity data. With few exceptions accumulations are predicted to lie in close proximity to areas of higher maturation. Using temperature isotherms the zone of potential present day biodegradation (40-80ºC) is predicted to extend from approximately 800 m to 1750 m (see also Figure 9). Predicted present day accumulations within this zone might therefore be affected by biodegradation and are marked accordingly in inset of Figure 6.

1.3.1 Source rock: extent and maturity

During subsidence of the trench source rocks are predicted to mature progressively (Figure 7 and Figure 8). Active source rocks are all older than 12 Ma, with the oldest (30 Ma) being the source of most of the generated hydrocarbon. Expulsion of hydrocarbon started 15 or 8 Ma ago depending on the assumed heat flow (Figure 7).
Source rocks were modeled as being widely distributed both in depth and in lateral extent. The Prometheus H-68, the Pluto I-87, and the two Zeus wells drilled a number of layers with low to moderate values of TOC. On the basis of these observations the PSM was constructed to contain three Tertiary source layers over depths ranging from 2500 to 6000 m.
In general Tertiary source rocks in the Tofino Basin are considered to contain primarily terrestrial, gas-prone type III kerogen and bulk kinetics according to Burnham (1989) were used during the modelling to describe its maturation behaviour. Subsidence is predicted to mature source rocks progressively. Calculated present day transformation ratios vary from 0-100% with the youngest source rock only maturing into the oil window under the assumption of the highest heat flwo tested for (80mW/m^2).

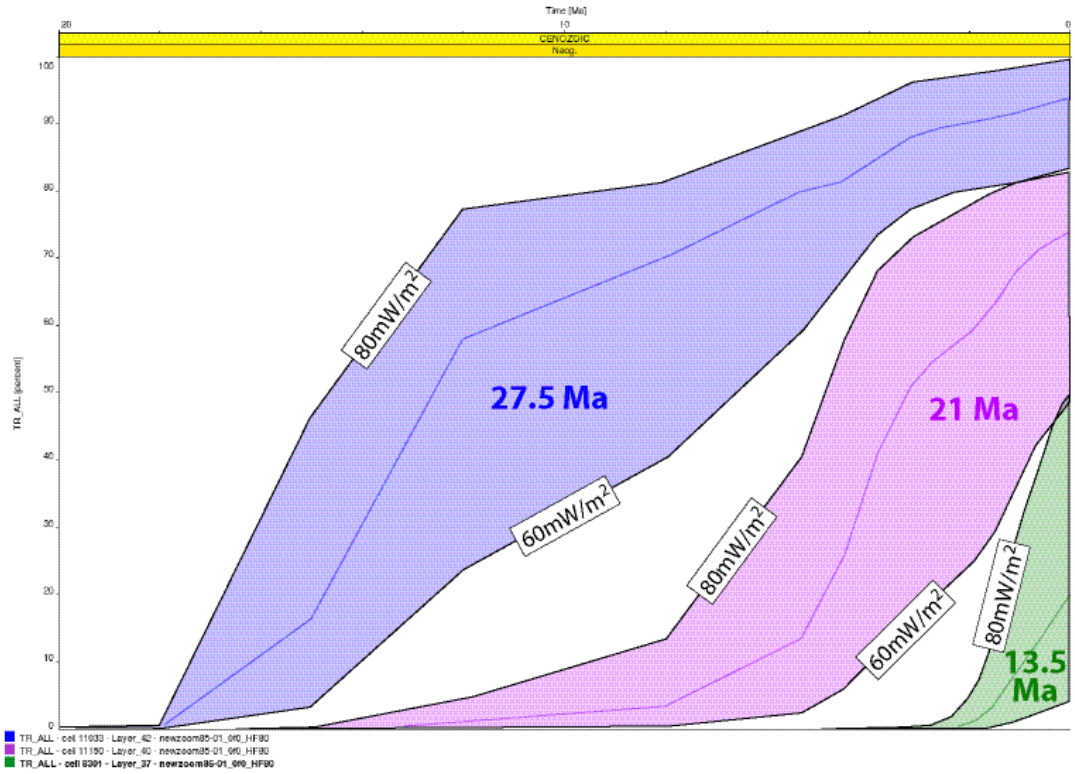

Figure 7. Variation of transformation ratio over time predicted for three Tertiary source rocks at their deepest burial along Line 85-01 depending on assumed heat flow.

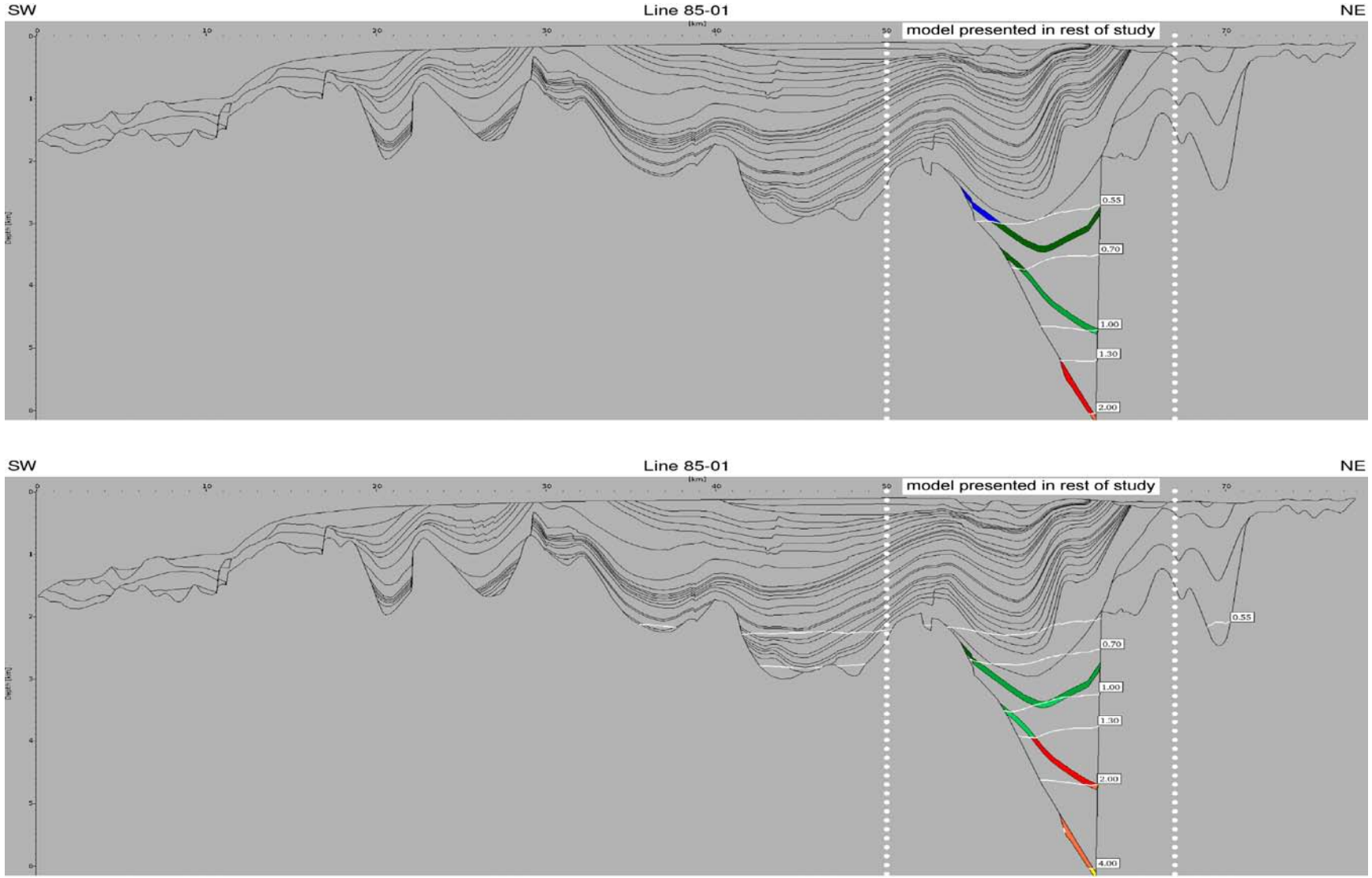

Figure 8. Predicted present day maturation level of Tertiary source rocks along line 85-01 assuming a constant heat flow of 60mW/m² above and 80mW/m² below. Results presented in the remainder are restricted to the area in between the white dotted lines as sediments outside are predicted to not have matured enough to generate hydrocarbon.

1.3.2 Migration

Migration of Tertiary gas was calculated to be vertical, either up faults or focussed into anticlines. In our 2D PSMs lateral migration up faulted monoclines also occurred, but rarely over distances greater than 10 km (Figure 9). This number could however be exceeded in reality as flow might continue out of the model plane of our 2D model. Hydrocarbon moving though the inter-layered silty–sandy sediments tended to do so in stages: saturate a porous layer, build up pressure, leak vertically, flow to the next porous layer, saturate it etc. Numerous stacked traps are predicted to occur either adjacent to faults or in anticline structures. Enhanced migration along fault planes results in lesser accumulations and more gas may have been lost to the surface.

1.3.3 Trapping

Vertical flow, vertically distributed source rocks and inter-layered sediments cause stacked accumulations under unconformities, along faults, in anticlines, or in stratigraphic traps (Figure 9). Most traps start to fill soon after onset of generation but their persistence depends on whether they were affected by draining faults.

In general, models without or with faults closed to migrating hydrocarbons show more accumulated hydrocarbon than models with faults open to migrating hydrocarbons because many of the faults provide pathways into sandy younger strata enabling hydrocarbon loss to the surface. Nevertheless, some traps are predicted to occur in anticlines fed, but not cut by faults. Most of the accumulations are below the zone of predicted biodegradation (Figure 9).

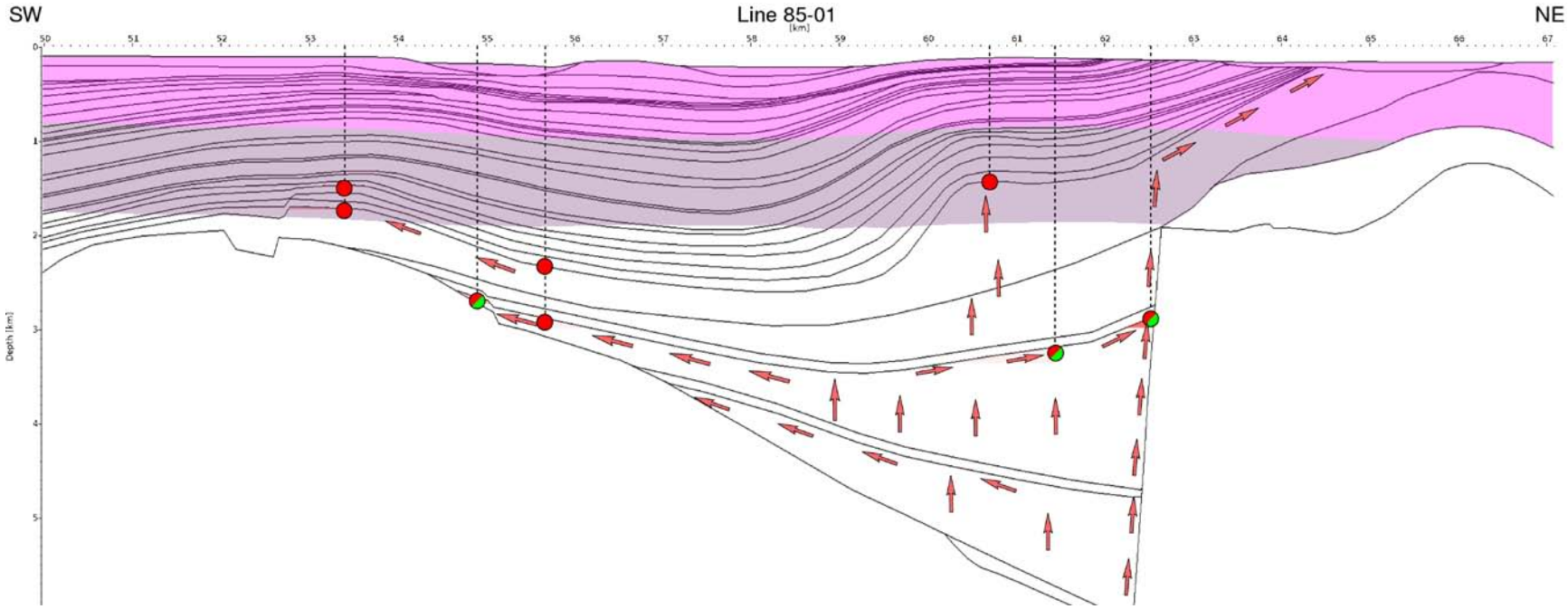

Figure 9. Hydrocarbon accumulations predicted to form in the vicinity of the deep trench imaged on Linel 85-01 averaging all calculated heat flow scenarios. Stacked accumulations(red: gas, green: oil) are predicted to have formed in shallow anticlines at 53 and 55 km, over the deepest part of the trench (60.5 km), and along the trench bounding fault (62.5 km). To assess possible influence of biodegradation predicted temperature intervals 0-40C (pink) and 40-80C (purple) are overlain. With the exception of the shallow anticlines most of the remaining accumulations were below the zone of predicted present day biodegradation.

1.4 Recommendations

To fully address the non-renewable conventional petroleum resource potential of the Tofino Basin the Petroleum Systems Modeling should be extended to include the trench sections of lines 89-01 and 89-06 that lie within the area. By doing so better estimates could be given regarding the extension of the oil/gas kitchen.
Addressing some of the most influential factors of the investigated petroleum systems might improve on the quality of resource predictions presented here. These are:

- *Kinetics of Tertiary kerogen*
  It would be beneficial to investigate the kerogen kinetics of the Tertiary source rocks in more detail. Kerogen kinetic strongly influences timing and type of generated hydrocarbon. Better knowledge of kerogen kinetics, ideally available as multi-component analysis, directly translates in more accurate predictions of type and location of hydrocarbon accumulations.

- *Improved mapping of sediment thickness*
  To allow for a meaningful lateral extrapolation of the results presented in this report an improved understanding of the sediment thickness over the whole Tofino Basin and especially the deep trench is required. Based on the already available seismic reflection data and ideally including new seismic reflection data such information could be extracted.

- *Permeability of Tertiary extensional faults*
  Our PSM has shown the strong dependency of predicted accumulations on hydrocarbon migration patterns. Migration is strongly influenced by distribution and character of faults. Predictions based on PSM could vastly improve if better knowledge of fault parameters such as permeability and changes of permeability with time could be achieved.

- *Possibilty of a Mesozoic sourced petroleum system*
  The Pacific Rim Complex underlying the Tofino Basin is composed in parts of Lower Cretaceous mélanges (Brandon, 1989) which comprises a mudstone-rich mélange (up to 55% black mudstones). Working petroleum systems sourced from equivalent rocks have been proven to the south in Washington and Oregon and inclusion of this older stratigraphy into PSMs might be attempted, although very limited available data today would be a severe handicap for such modelling.

Apart from the conventional non-renewable resources parts of the area might present conditions in favour of non-conventional gas hydrate resources (i.e. Hannigan et al., 2005), which are not addressed in this report.

2 Introduction

2.1 Previous work

Based on a simple geohistory/maturation model Bustin (1995) assumes Pliocene and younger strata to be immature and Lower Miocene and Oligocene strata (in the 1-87, 1-65 drill holes) mature with respect to the oil window. Bustin concludes, that maturation is consistent with a heat flow in the order of 50mW/m2 and thermal conductivity of about 2.0W/mK (Bustin, 1995). According to Hannigan the Tofino Basin region has a single defined play with a potential of 266 billion m^3 (9.4 TCF) of in-place gas. Forty-one fields with more than 3000 million m^3 gas volume are predicted to occur (Hannigan et al., 2001).

2.2 Geological backround

The Tofino Basin is a sedimentary forearc basin that formed following the accretion of the Crescent and Pacific Rim Terranes in the Eocene (Hayward & Calvert, 2007). The Tofino Basin is bound to the west by the continental shelf edge, and extends southeast from the Brooks Peninsula and Kyuquot Uplift to the Juan de Fuca Strait covering an area of over 25.000 km^2 (Narayan 2003). It overlies the Pacific Rim, Crescent terranes, and the modern sedimentary wedge to the southwest of Vancouver Island (Figure 1 and Figure 10) and the deformation of overlying Tofino sediments has been controlled by this basement composition.

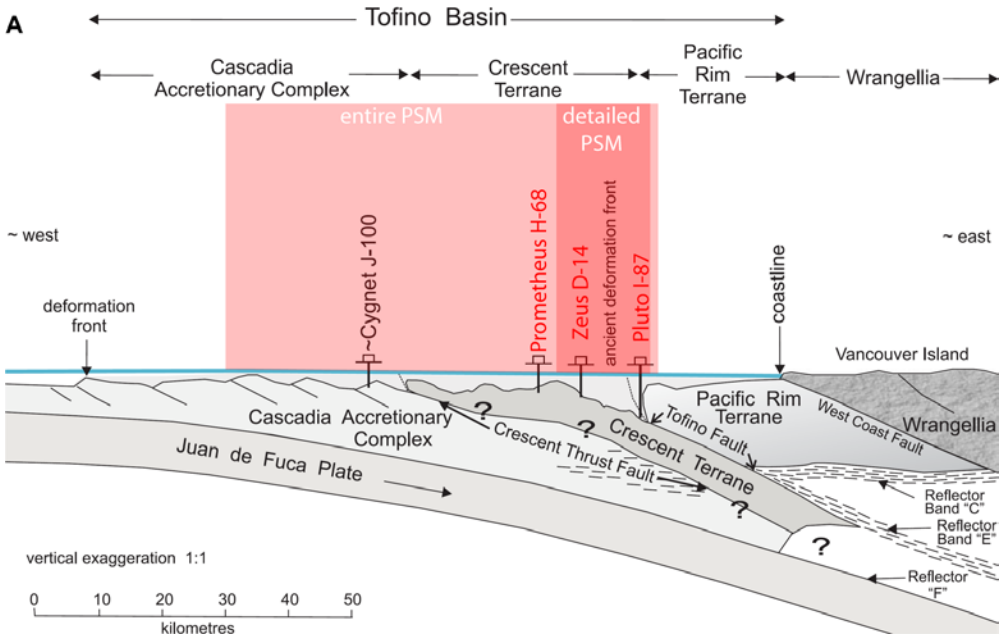

Figure 10. Schematic cross section of the Tofino Basin, based on work by Hyndman et al. (1990) (modified from Johns et al., 2006). Wells used for model construction and calibration are marked in red.

2.2.1 Stratigraphy

Recent biostratigraphic re-evaluation (Narayan 2003; Narayan et al. 2005) of Shell Canada's exploration wells allows to better constrain the basin development using the existing high quality seismic reflection data that was acquired by the Geological Survey of Canada in 1985 and 1989 (Yorath et al. 1987; Spence et al. 1991). The basin is comprised of Eocene to Holocene turbidites and hemipelagic sedimentary rocks (Hyndman et al. 1990; Yorath et al. 1987) with the dominant lithologies being mudstone, siltstones, minor lenticular and argillaceous sandstone, conglomerate and breccia (Shell Canada 1968a, b, c, d; 1969a, b; Shouldice 1971). Up to 6km of Oligocene to Holocene sediments are observed in a coast parallel sub-basin over the Tofino fault separating the Crescent and Pacific Rim terranes. Diapiric structures along its axis suggests fluid expulsion from the deeper accreted terranes. Some of the underlying crust seems to be continental and transitional and might include facies similar to the Mesozoic and older rocks on Vancouver Island (Haggart et al., 2003).

2.2.2 Structure

Together with the Pandora Peak and the Leech River schists the Pacific Rim Complex forms a set of "displaced Mesozoic rocks" outboard of the continental framework consisting of Wrangellia, the Coast Plutonic complex, and younger plutons that intruded the older terranes (Monger et al., 1982). The "displaced Mesozoic rocks" are internally separated and bound by much younger Eocene faults, leading Brandon (1989) to interpret them as displaced terranes rather than intact parts of a Jurassic –Cretaceous subduction complex. Based on stratigraphy and metamorphism Brandon (1989) proposes their formation on the inboard side of Wrangellia about 30Ma prior to its collision with the American continent.

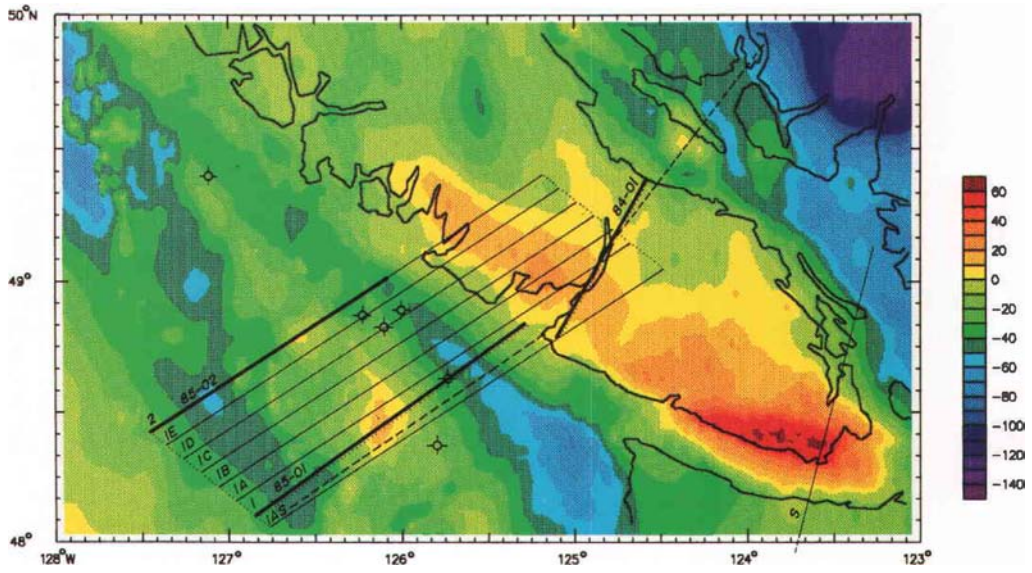

Figure 11. Gravity anomaly map (free-air at sea, Bouguer on land) from Dehler and Clowes (1992) that shows the extend of the deep sedimentary trench approximately 20km offshore (gravity low).

2.3 This study

2D petroleum systems modeling of the Tofino Basin presented in this study is entirely based on publicly available data. No isopach map is available for the region and extrapolation from the available 2D data was based on gravity data. Although preliminary, this approach allows to determine the general shape and location of the Neogene filled trench (Figure 6 and Figure 11). Reflection seismic data collected by the Geological Survey of Canada (GSC line 85-01) in 1985 was employed to determine the models geometry.

Well reports providing stratigraphic and lithologic information in combination with state of the art petroleum systems modeling software, allowed source maturation, hydrocarbon migration and entrapment to be modeled. While many of the parameters fed into the model remain unknown for this frontier basin, this report sheds light on the interaction of processes and which of the estimated variables are most crucial to study in future exploration.

3 Input data

3.1 Reflection seismic

Seismic reflection line 85-01 was collected by the GSC in 1985 and was shot SW-NE spanning the entire Tofino Basin as well as part of the deeper offshore west of it (Figure 12). Conversion of the seismic data to depth is based on velocity profiles constructed from check shot surveys at the wells. Individual check shot data were used to fit a Vo + kZ function to each well from the water bottom. Water was assigned a constant velocity of 1480 m/sec and velocity functions were interpolated over the region, based on a weighted sum of the control points near the desired location. A normalized inverse distance weighting scheme with a search range including at least three data points was used. Average depth errors at the wells were < 50 m. Depth prediction errors at non-well locations were somewhat greater than this. The velocity model was tied to the wells using large radius Gaussian functions followed by short radius inverse distance operators. At the wells the depth errors then averaged to < 10 m. The model assumed that only sediments were present so if volcanics are interbedded with sediments in the very deepest sub-basins, the depths may be under-estimated. However, at these depths, the projected velocities of the sediments should begin to converge with the average velocities of the volcanics so there should not be a large error. Depth projections of reflections from Mesozoic rocks below the basin may have larger errors.

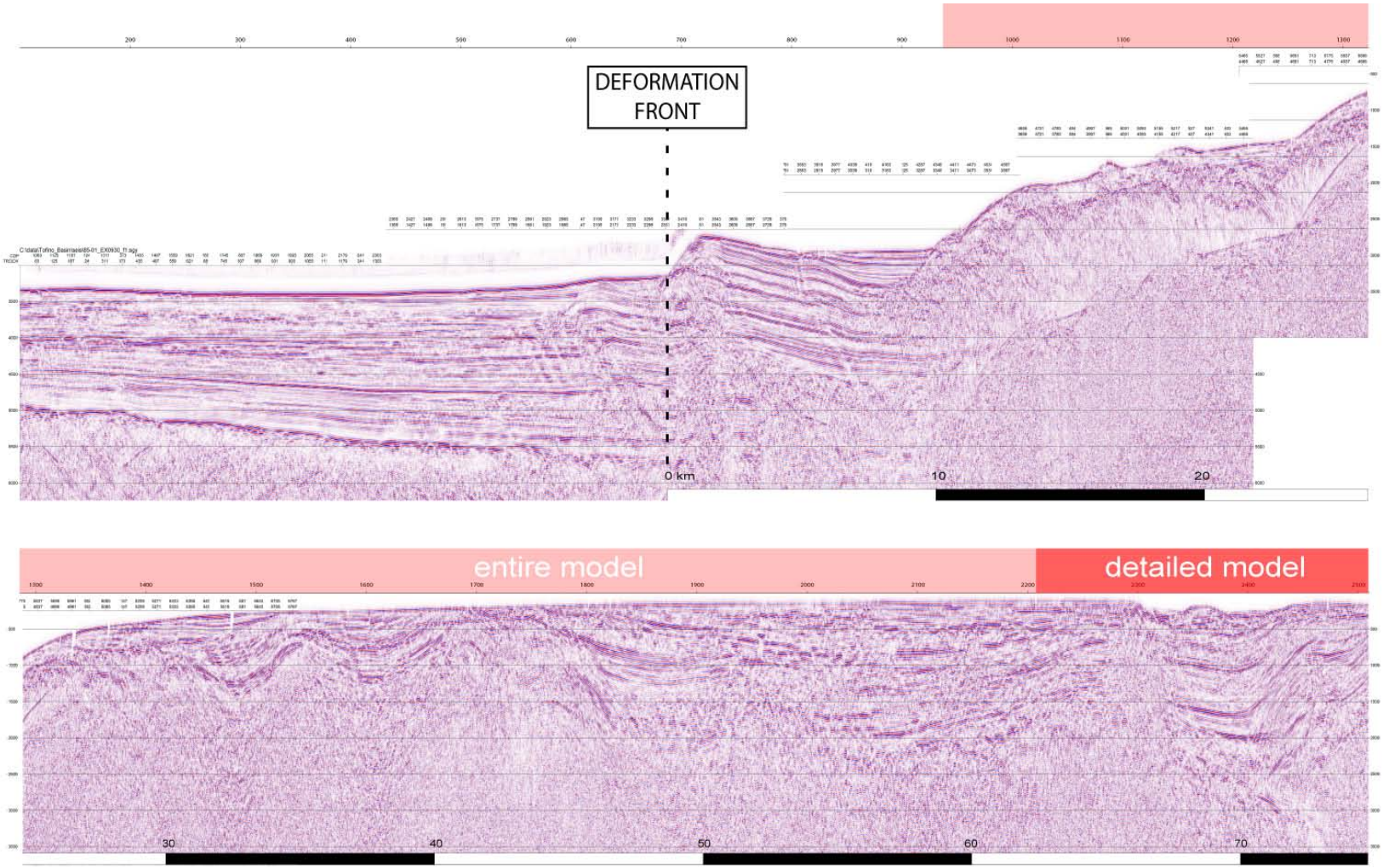

Figure 12. Reflection seismic data 85-01 with deformation front and extend of PSMs marked.

3.1.1 Stratigraphic units

Multiple wells have been drilled in the offshore and allow a characterization of the main stratigraphic units and their lithologies within the Tofino Basin infill. For the modelling the units were defined based on variations in well lithologies and simply given consecutive numbers for identification. The Oligocene is represented by units 42-40, the Miocene by units 39-35, the Pliocene by units 34-25, the Pleistocene by units 24-20, and the Holocene by units 20-1. The sediments filling the deep trench (units 42-35) are all older than 5.3Ma and not represented outside of the trench. Underlying basal reflectors are of lower frequency, intermittent and partly of high amplitude and were treated as economic basement during this study.

Lithology was assigned to each interval following correlation of seismic to well data. Necessarily some layers were lumped together but the general character of sandstones interbedded with siltstones was preserved. Physical parameters such as porosity and permeability were assigned using generic curves provided by the software based on percentage of sand, silt, etc assigned to individual intervals (see Figure 13).

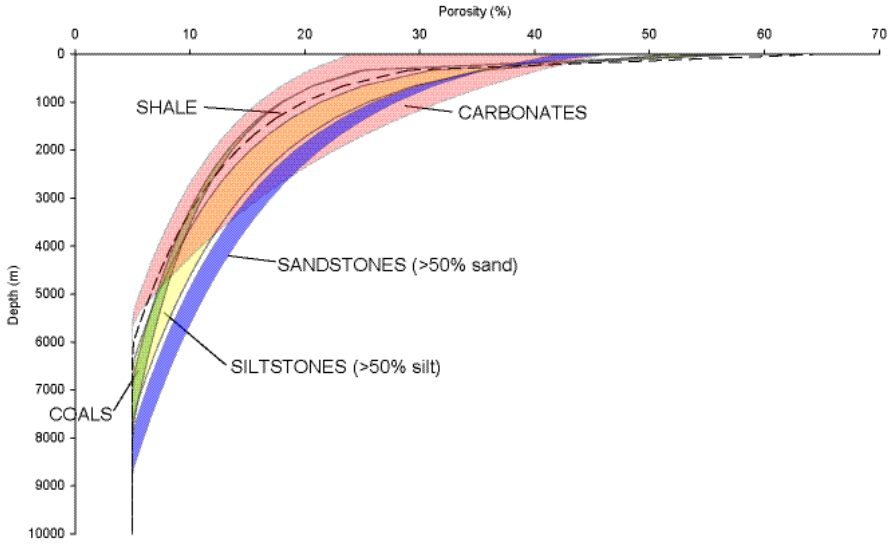

Figure 13. Compaction as function of burial depth for different lithologies used in the 2D modeling.

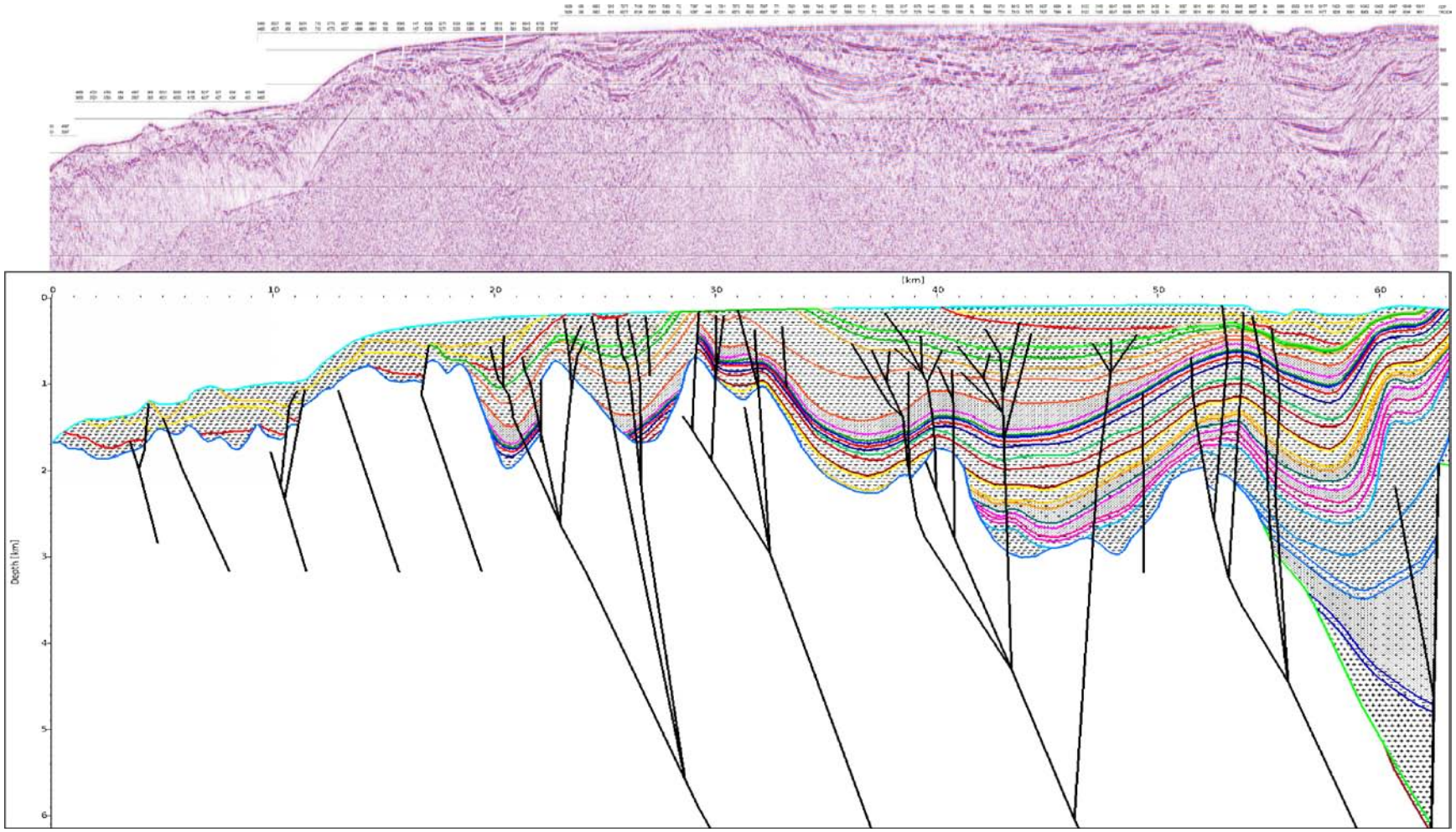

Figure 14. Reflection seismic image of the modelled part of GSC Line 85-01 (above) with model interpretation (below). Note: Reflection seismic image is presented in time domain, whereas model shows interpretation converted to depth.

3.1.2 Source rocks

Bustin (1995) characterized the Tofino strata as overall low in total organic carbon content (avg. = 0.8%) and low hydrogen index (avg. = 80 mg HC/g TOC), see Figure 15. The kerogen present is predominately terrestrial (type III) and mainly comprised of finely divided vitrinite. Bustin (1995) reports poor source rock qualities with the richest intervals to occur in Miocene and Oligocene strata as encountered in the D-14 and 1-87 wells. Pliocene and younger strata is immature and maturation estimates from Tmax and vitrinite reflectance place place the top of the oil window below the depth reached in all but the I-65 and I-87 wells, where Lower Miocene and Oligocene strata are mature with respect to the oil window (Bustin, 1995). Shallow gas has been recoded in I-87 and H-68 wells (Bustin 1995 citing Shouldice, 1973).

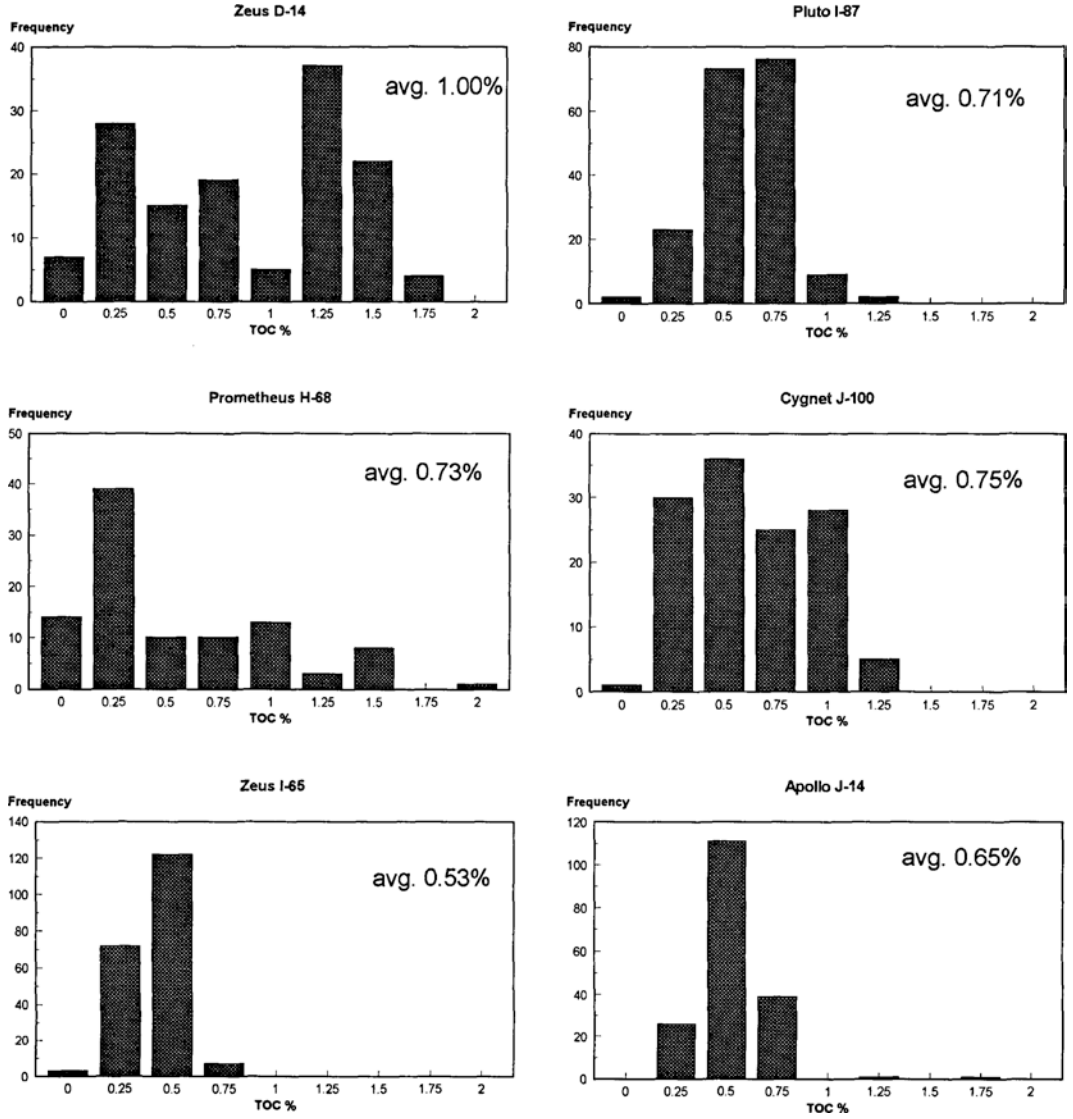

Figure 15. Distribution of Total organic content (TOC) measurements from the six Tofino Basin offshore wells (Bustin, 1995).

Bustin (1995) used cross-plots of the hydrogen and oxygen indexes (Figure 16) and determined the dominant kerogen type in the Tofino Basin as Type III (HI <300 mg HC/g Corg). The production index [S1/(SI+S2) from Rock-Eval] and the overall TOC content of sediments in the Tofino Basin is low with an average of only 0.8%, and very few samples have TOC values greater than 1.5% according to Bustin (1995). Characteristics of hydrate bound and vent gas from Barkley Sound also infer a thermogenic source comprising of mainly type III with a small fraction of type II kerogen (Pohlman et al., 2005).

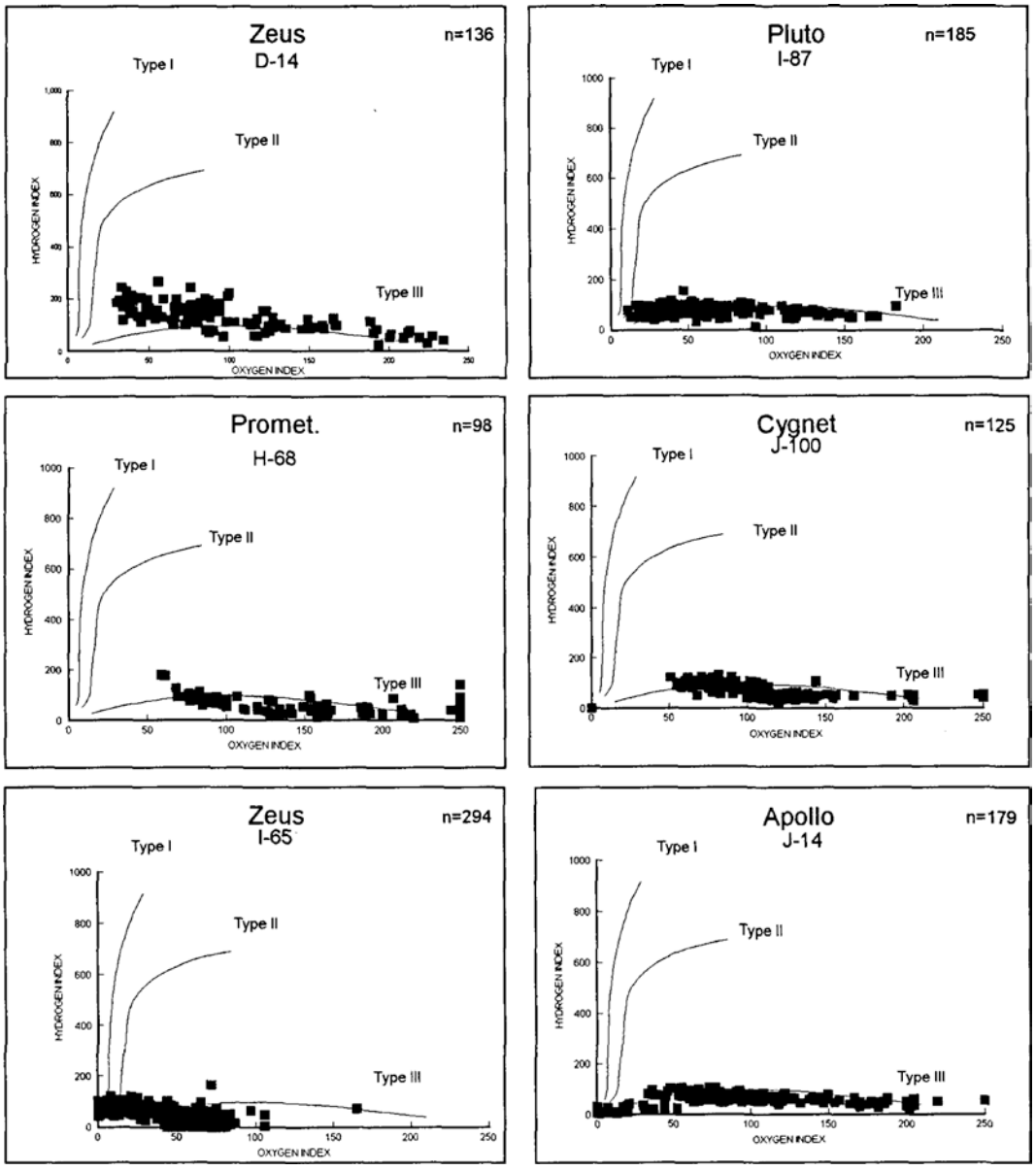

Figure 16. Cross-plots of the hydrogen and oxygen indexes for the six offshore Tofino Basin wells (Bustin, 1995). All kerogen encountered can be categorized as type III.

Kerogen in the Tofino Basin occurs in many thin layers and modelling of each individual layer is beyond the possible resolution of the 2D models. Three representative source rock layers were modeled to account for elevated organic content in the Oligocene and Miocene. As a general assumption source rocks within the Tofino Basin are assumed to be lacustrine of terrestrial origin. Bulk kinetics according to Burnham (1989) were chosen to be used throughout the Tertiary section and source rock character was assumed to be laterally homogeneous over the region studied.

Reservoir quality of Shouldice (1971, 1973) described the deep water succession (outer neritic to midbathyal,) as having a poor overall reservoir quality which is in accordance to Bustin considering the poorly indurated, interbedded light- to dark-coloured mudstones, siltstones and rare fine-grained sandstones a poor reservoir due to no or little porosity and common clay matrix/cement (Bustin, 1995).

3.1.3 Faults

Faults and their permeability are integral to assessment of the hydrocarbon potential of this basin and three scenarios with respect to fault permeability were identified and tested for during the petroleum systems modeling (faults not present, faults open for migrating petroleum, faults closed to migrating petroleum).

4 Calibration

Calibration data are sparse, with only one well (Pluto I-87) drilled deep enough into the investigated trench in the Tofino Basin. Vitrinite reflectance derived from Tmax measurements provide the best calibration available (Bustin, 1995, Dewing & Sanei, 2009). With stratigraphy and burial given the heat flow remains as the main parameter for calibration of our models to maturation data available through studies of bottom simulating reflectors (BSR) and Tmax and Vitrinite reflectance values derived from well sites.

4.1 Heat flow data

Heat flow data are available from land boreholes and petroleum exploration wells on the continental shelf (Lewis et al., 1988, 1991), marine probe measurements on the continental slope and Cascadia Basin (Davis et al., 1990; Hyndman et al., 1993; Spence et al., 2000b; Riedel, 2001; Riedel et al., 2006), and from the depth of the BSR on the continental slope (Hyndman et al., 1993, 1992; Ganguly et al., 2000; Riedel, 2001; He et al., 2003).

The young age of the oceanic lithosphere (8-6 Ma) causes high heat flow of about 140mW/m^2 in the western part of the Tofino assessment area, while heat flow decreases landward across the continental margin to about 60 mW/m^2, due to subduction of the oceanic lithosphere (Langseth and Hobart, 1984; Davis et al., 1990, Wang et al., 1994). The initial decrease is accentuated by the tectonic thickening of the accretionary wedge. This decrease in heat flow landward due to the landward deepening of the oceanic plate and thickening of sediments at the accretionary wedge has been described and modelled by Hyndman & Wang, 1993, Hyndman et al., 1994, and Wang et al., 1995 (see Figure 17). Davis et al. (1990) recognized a general trend with heat flow decreasing landwards across the continental margin from an average of 120 mW/m2 in the Cascadia Basin, to about 90 mW/m2 over the lower continental slope, to about 50 mW/m2 at the continental shelf.

More recently Ganguly et al. (2000) observed a similar regional trend in the Tofino Basin with heat flow decreasing landward across the margin from an average of 80 mW/m2 at a distance of 15 km from the deformation front to 65 mW/m2 at a distance of 40 km. All these values are in agreement with the predictions for 6 Ma old oceanic crust according to Parsons and Sclater (1977) and accounting for a reduced heat flow as a consequence of horizontal shortening and thickening of the sediment section that vertically stretches the isotherms faster than thermal re-equilibration can occur (Hyndman and Wang, 1993; Wang et al., 1993). Ganguly et al. (2000) projected heat flow values along a multiple profiles on to a line perpendicular to the margin finding an average heat flow value for the region between 70 and 80 mW/m2 (Figure 17).

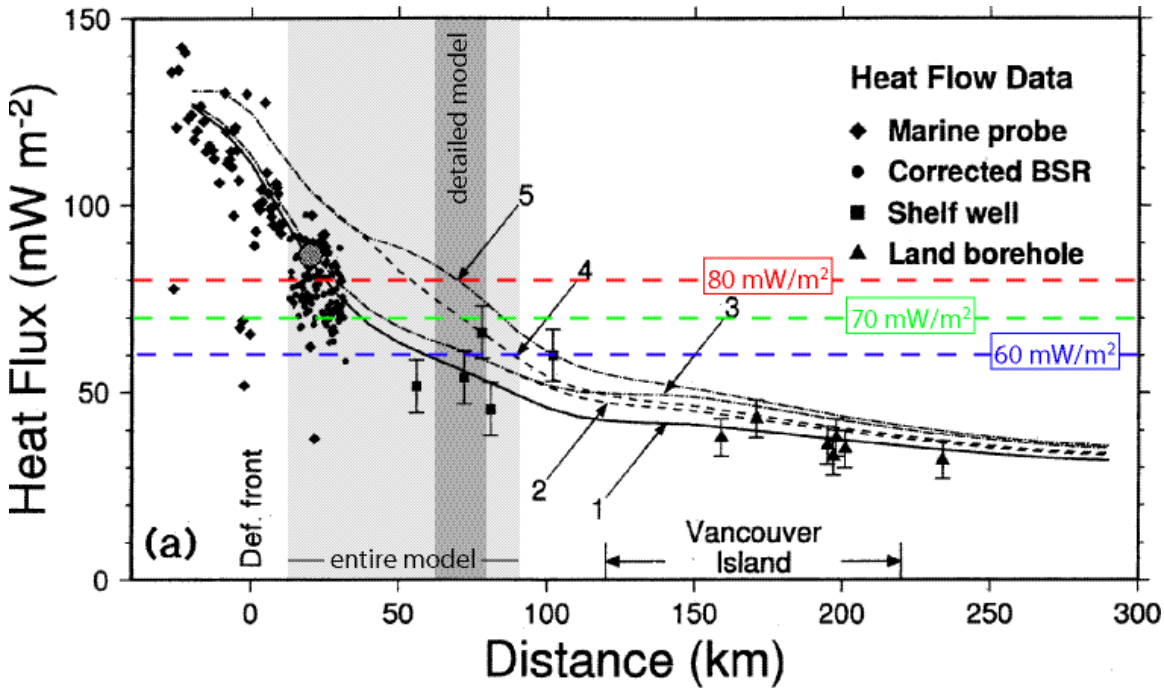

Figure 17. Heat flow profile across the Tofino Basin and Vancouver Island. The three scenarios used during this study are marked. They cover the span of uncertainties based on the various methods of determining heat flow.

4.2 Bottom simulating reflectors (BSRs)

Along the Cascadia Margin seismic records indicate widespread occurrence of BSRs several hundred meters beneath the seafloor in continental slope sediments, particularly in the accretionary wedge of the subduction zone (Shipley et al., 1979; Kvenvolden and Barnard, 1983). Massive hydrates have been recovered in Deep Sea Drilling Project (DSDP) cores from sections above BSRs (Kvenvolden and Barnard, 1983; Suess et al, 1988) and methane derived CO_2 has been described in pore fluids (Suess et al., 1989).

Inferred temperatures at BSRs provide an important reference for the mapping of geothermal gradient and heat flow from accretionary wedges (Hydman et al., 1992). BSR temperatures at three sites (Nankai, Peru, and Blake Ridge) are in the order of 25-27 ± 2°C. BSRs are commonly found beneath the lower to mid-continental slope at depth of several hundred meters and are taken to mark the base of temperature-pressure stability field for methane clathrate hydrate. As its stability is only moderately dependent on pressure and pressure can readily be estimated a temperature reference is given.

Thermogenic gas hydrates mainly consist of methane but contain significant quantities (>1%) of C_2-C_5 hydrocarbons formed by thermal pyrolysis of fossil organic matter (Brooks et al., 1984; Sassen & MacDonald, 1994). Thermogenic gas hydrates have been reported from the Gulf of Mexico, the Caspian Sea, the southern summit of Hydrate Ridge offshore Oregon, and the northern Cascadia margin offshore VI, where its composition of primarily methane (65.1% to 85.1%) with significant quantities of

thermogenic C_2-C_5 hydrocarbons identified it as thermogenic in origin (Pohlman et al., 2005).

4.3 Vitrinite reflectance

Vitrinite reflectance data from the Tofino Basin wells is of generally poor quality and Tmax measurements provide much more reliable maturation indicator for the Tofino Basin, according to Bustin (1995). In combination with a fairly homogenous kerogen type (type III) and Rock-Eval S2 values greater than 0.2 mg HC/g rock Tmax values can be converted into equivalent vitrinite reflectance values with the oil window defined between 435 and 465°C *(*Espitalé *et al.*, 1985, Dewing & Sanei, 2009).

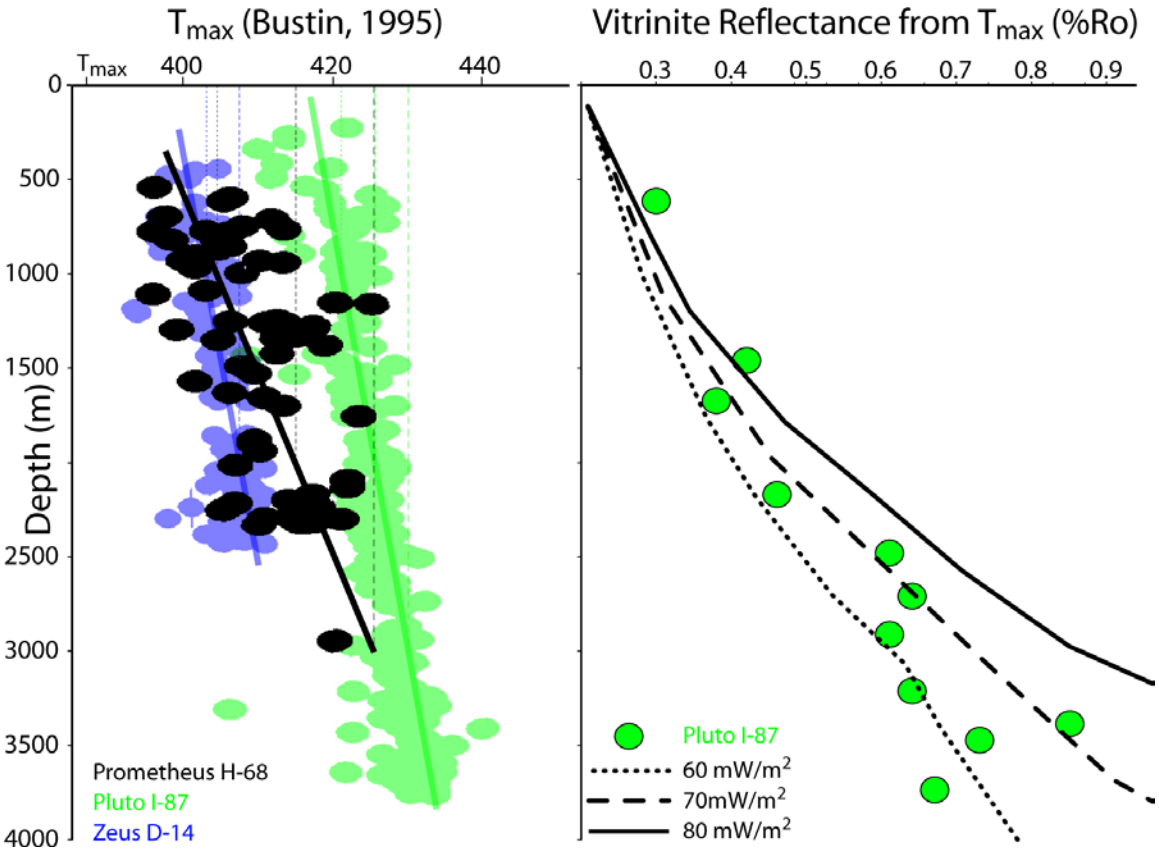

Figure 18. Left: T_{max} as measured for the Tofino Basin wells by Bustin (1995). Right: Vitrinite reflectance (%Ro) derived from T_{max} values using correlation presented in Dewing & Sanei (2009) for type III kerogen. Only the values for the Pluto I-87 well are shown, as it is the only well drilling deep enough. Calibration for the three scenarios tested are shown.

5 Results

Few accumulations originating from Tertiary source rocks are predicted to exist along Line 85-01 (Figure 23). However, near continuous generation of hydrocarbon since the upper Miocene filled structural and stratigraphic traps where predicted. When faults were assumed to be permeable they allowed leakage, leading to loss of petroleum to the seafloor with the remaining accumulations existing in a steady state being refilled through ongoing petroleum generation while drained simultaneously. The predicted accumulations are of very minor scale. Oil generation from the gas prone terrestrial sources is very minor and only plays a role in the coolest of the investigated scenarios. Gas/oil generation from Tertiary terrestrial/marine source rocks commenced approximately 15 -8 Ma ago depending on the assumed heat flow scenario and continues today.

5.1 Structure and stratigraphy

GSC line 85-01 images a prominent Eocene sedimentary trench in the Tofino Basin paralleling the coastline approx. 20km off shore (Figure 10 and Figure 30). Well control is available via the Prometheus H-68 and projected Pluto I-87 and Zeus D-14 wells. Tertiary sediments are generally thin with the exception of the above mentioned trench, where they reach over 5 km in thickness. A minor inversion overlying the trench (60.5 km) unaffected by faults created the most persistent, if small petroleum trap as all others were strongly affected by differences is assumed fault permeability (55.5, 61, and 62.5 km).

5.2 Maturation

Three tertiary source rocks were assumed to be distributed vertically from 2500 to 6000 m, ranging in age from 12 to 30 Ma. No younger/shallower source rocks were included in our models, as their maturation would not have been sufficient for the generation of any hydrocarbon. Gradual subsidence allowed these source rocks to mature progressively and generation is calculated to be ongoing for the last 8 Ma or 15 Ma, assuming a heat flow of either 60 or 80 mW/m² (Figure 19). Transformation ratio varies with burial and assumed heat flow but kerogen in the deepest source rock has generally been transformed to over 80% (Figure 20 and Figure 21).

Depth to predicted transformation ratio values >50% for Tertiary source rocks varies from approximately 3200 to 5000 m. The youngest source rock achieved a maximum transformation ratio of less than 50% even in the 80mW/m2 scenario and does therefore hardly contribute to the petroleum system (Figure 20).

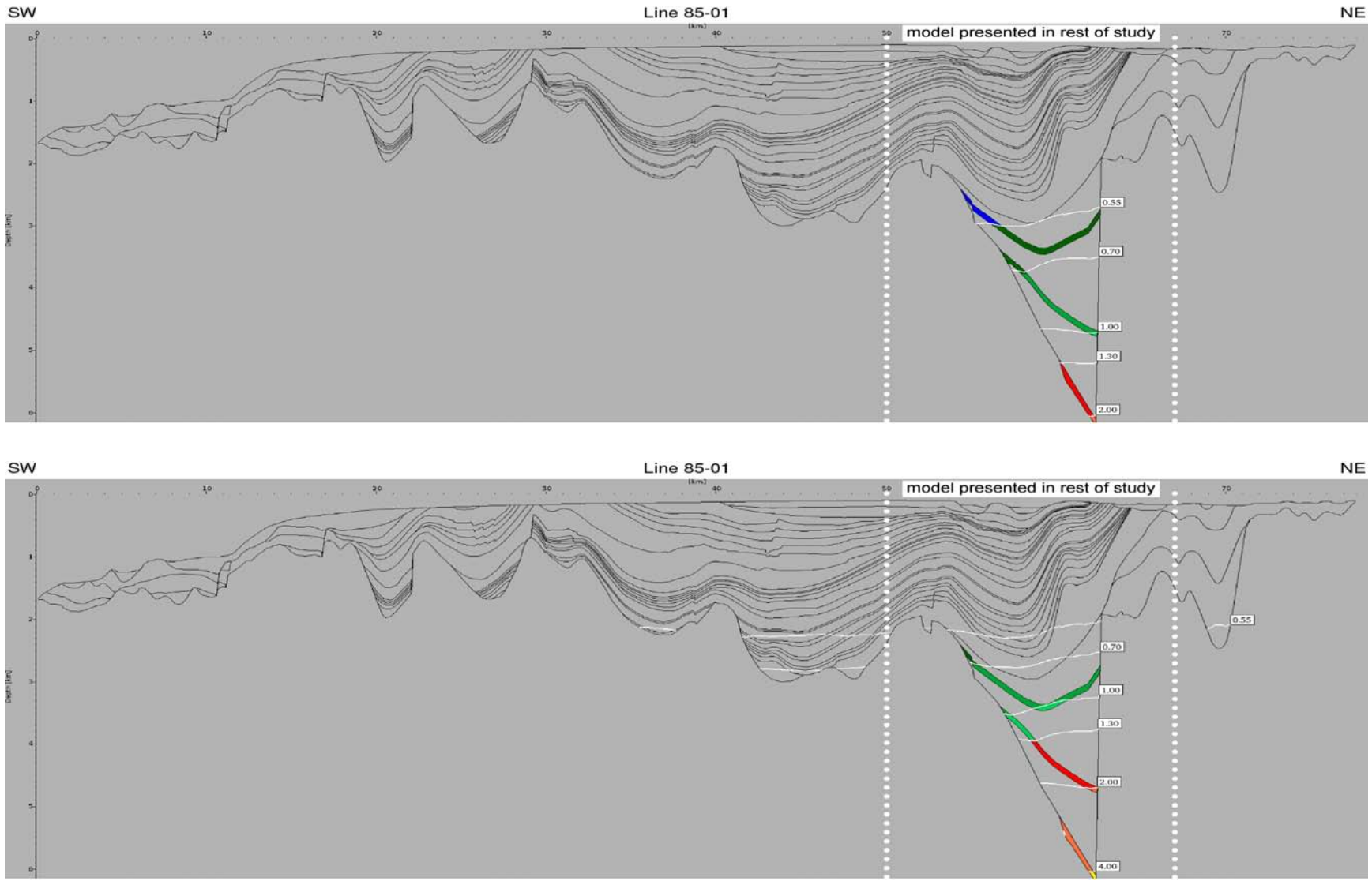

Figure 19. Predicted present day maturation level of Tertiary source rocks along line 85-01 assuming a constant heat flow of 60mW/m² above and 80mW/m² below.

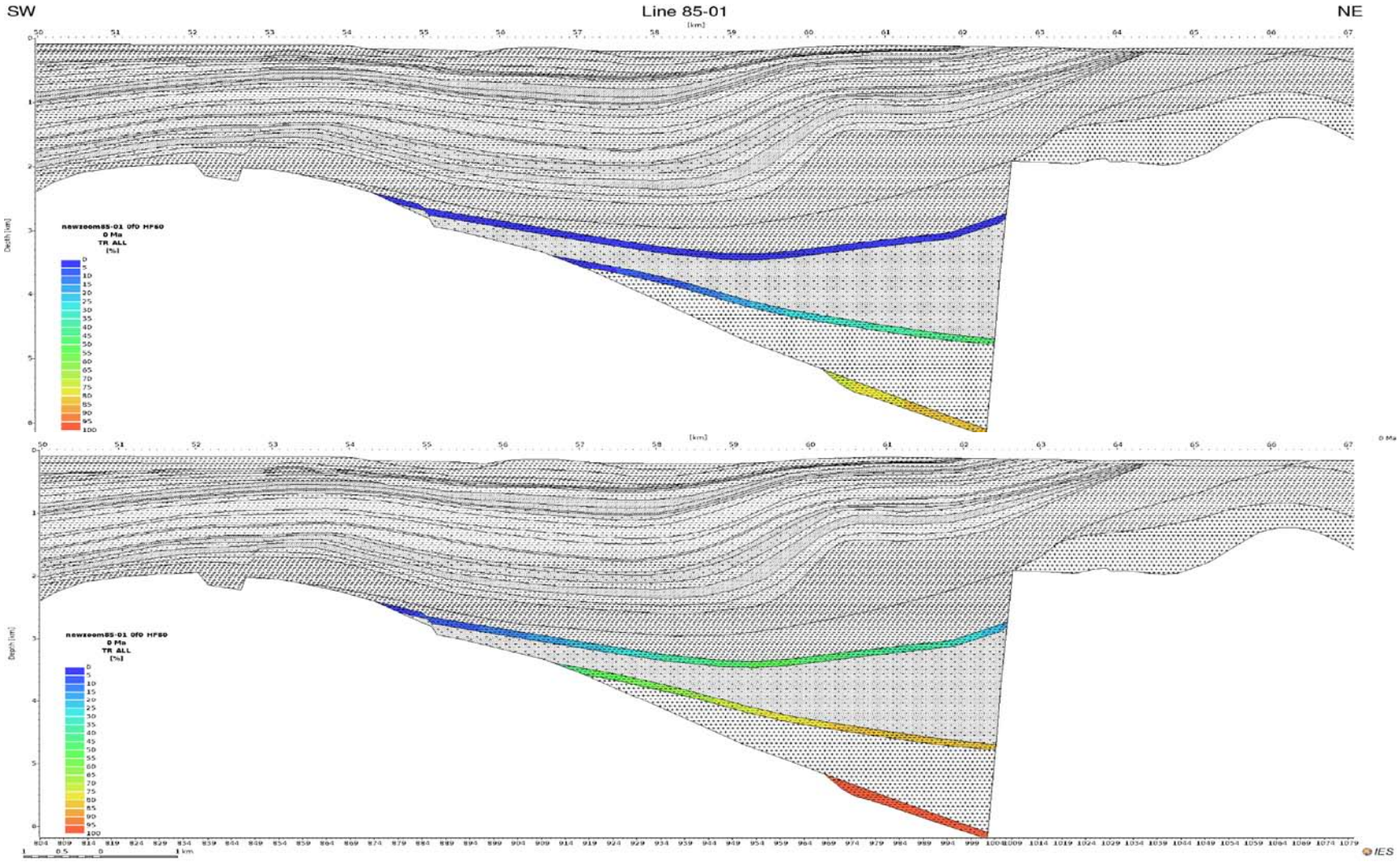

Figure 20. Predicted present day transformation ratio of Tertiary source rocks along line 85-01 assuming a constant heat flow of 60mW/m² (top) and 80mW/m² (bottom). Plot of transformation ratio over time presented in Figure 21 refers to deepest part of the trench at 62km.

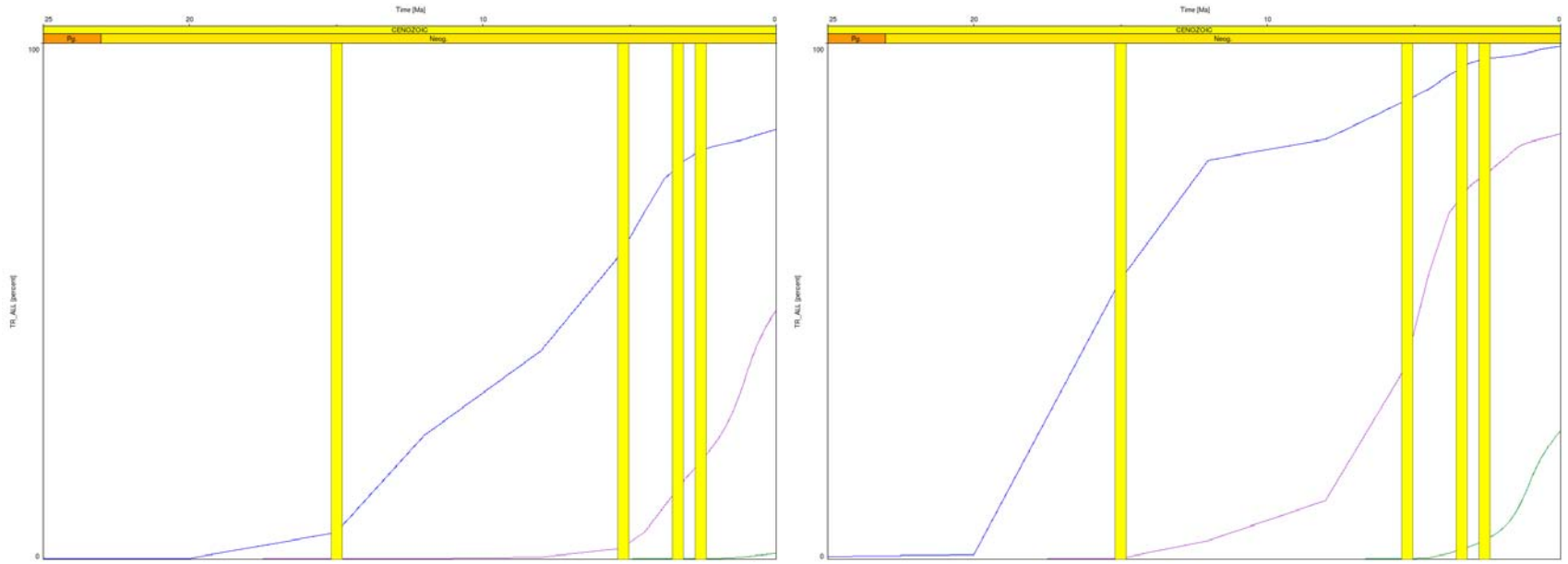

Figure 21. Transformation ratio over time for various source rocks in the deepest part of the Eocene trench (62km, see Figure 20 for location). Yellow bars mark deposition of main reservoir intervals Left: 60mW/m², Right: 80 mW/m².

Evolution of transformation ratio and deposition of reservoir strata are depicted in Figure 21 for the deep Eocene trench on line 85-01. The main phase of transformation of the deepest Tertiary source rocks is predicted to start ~15-8 Ma ago, depending on the assumed heat flow. Generation of hydrocarbon continues until present day. Multiple reservoir strata are in place by the time the younger source rocks are transformed into petroleum.

5.3 Migration and trapping

Migration was focused into anticlines, along faults and up dipping layers (Figure 23). Faults when assumed to be permeable drained adjacent traps, redistributing the gas into younger units where they might be trapped in inversion structures overlying the deep Eocene trench (53-62 km). In general more traps are predicted to be filled when fault were assumed sealing, otherwise petroleum was likely lost to the surface.

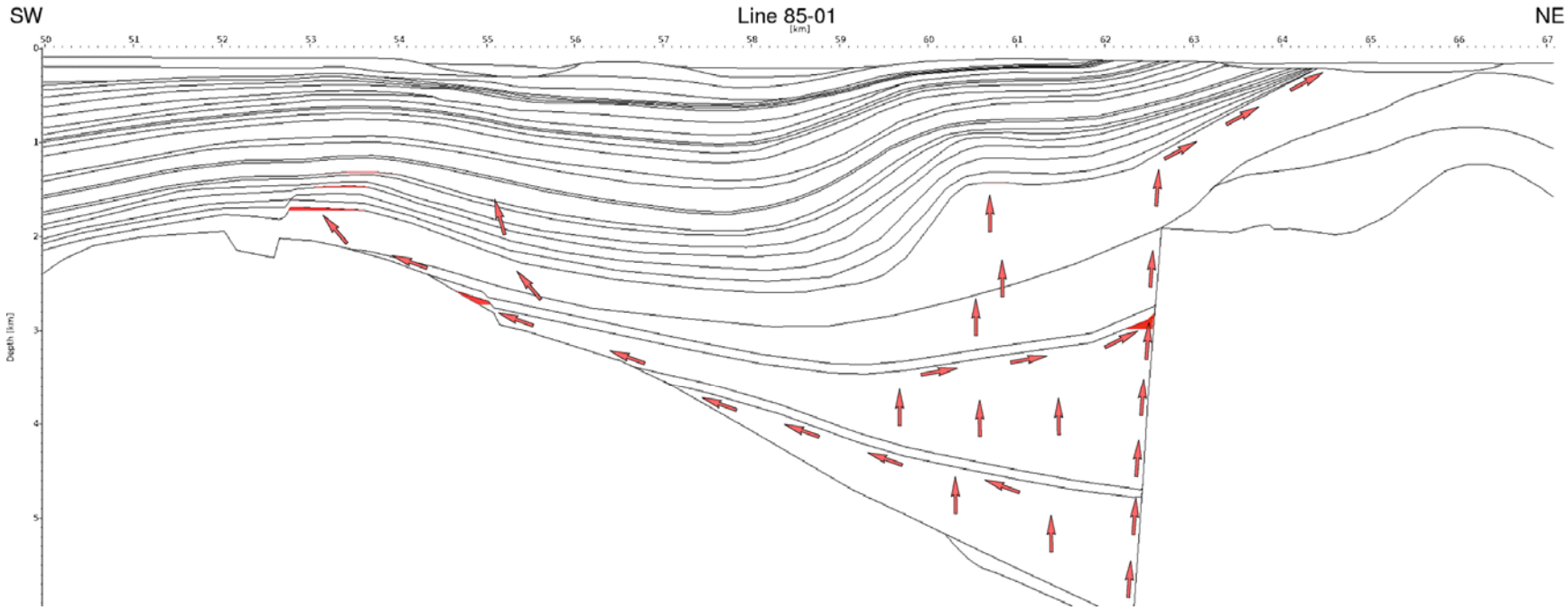

Figure 22. Predicted gas accumulations along line 85-01 averaged over all scenarios calculated. Intensity of colour was determined by number of occurrences, according to modelled scenarios. Arrows represent main migration pathways.

.

The two most consistently predicted accumulations form under an anticline structure and adjacent to the near vertical fault east of the Eocene trench. Migration pathways into these accumulations show the dominance of vertical as opposed to lateral migration. Maximum distance of lateral migration is predicted to be less than 8 km (Figure 23).

5.4 Evolution of main accumulations and possible biodegradation

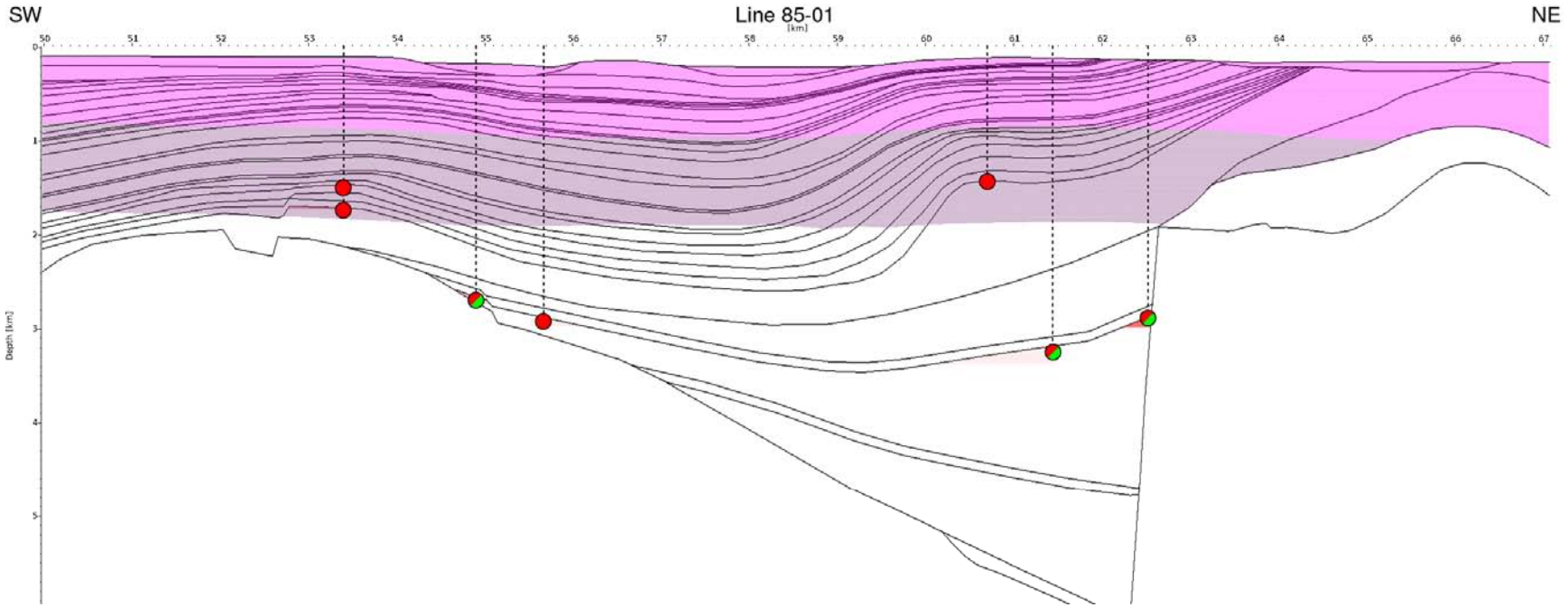

Figure 23. Zone of possible present day biogenic gas formation (pink: 0 - 40°C) and biodegradation (purple: 40 - 80°C) along line 85-01 outlined by temperature field resulting from a heat flow of 70mW/ m² superimposed onto predicted accumulations as presented in Figure 23. Six locations are marked at which 1D pseudo well extractions have been used to visualize history of accumulations and potential influence of biodegradation (Figure 24 to Figure 29).

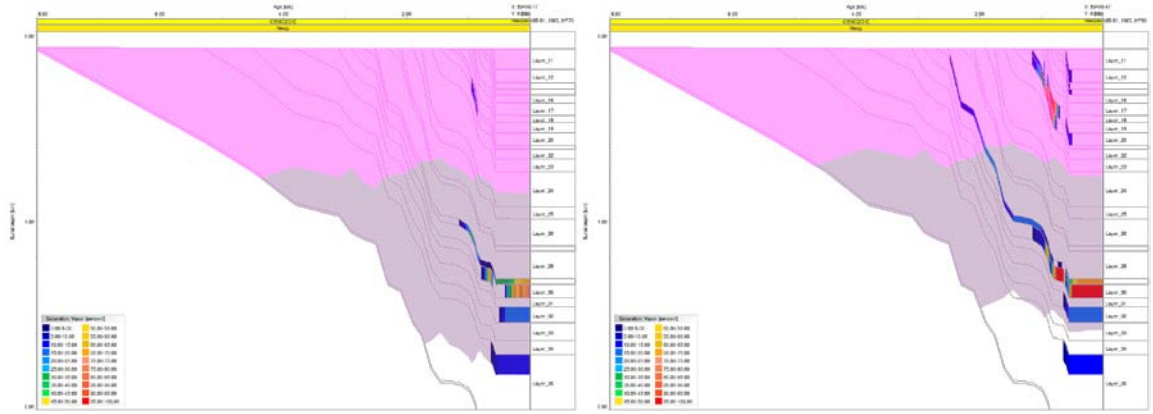

Figure 24. Hydrocarbon saturation over time in a pseudo well located 53.5 km from the south western end of line 85-01 (left: 70mW/m², right: 80mW/m²). To assess biodegradation temperature field is indicated by colour overlay as in Figure 23. No faults. Note: No accumulations were predicted for this location assuming a 60mW/m² scenario.

Predicted accumulations at 53.5km from the south western end of line 85-01 are very likely to have experienced biodegradation in the past and today, possibly degrading the quality of the trapped petroleum.

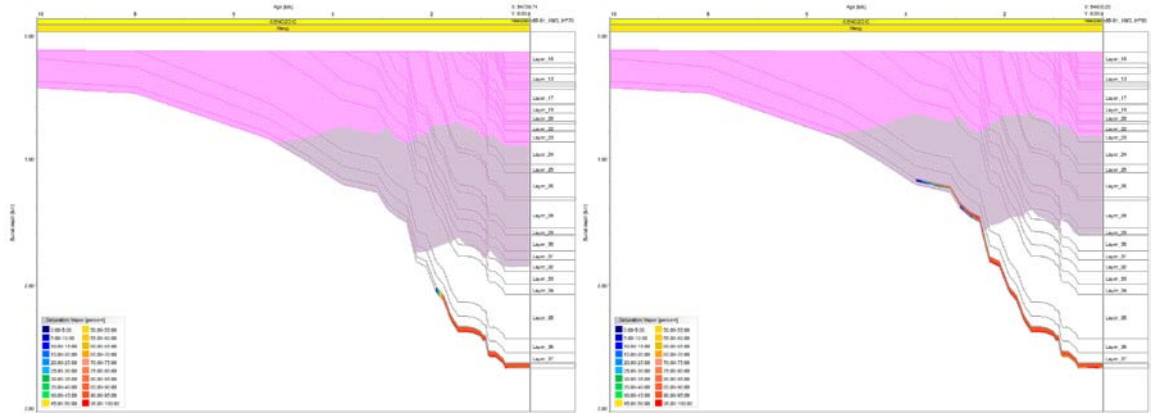

Figure 25. Hydrocarbon saturation over time in a pseudo well located 54.8 km from the south western end of line 85-01 (left: 70mW/m², right: 80mW/m²). To assess biodegradation temperature field is indicated by colour overlay as in Figure 23. No faults. Note: No accumulations were predicted for this location assuming a 60mW/m² scenario.

Predicted accumulations at 54.8km from the south western end of line 85-01 lie deep enough to have not been affected by biodegradation in the past and today.

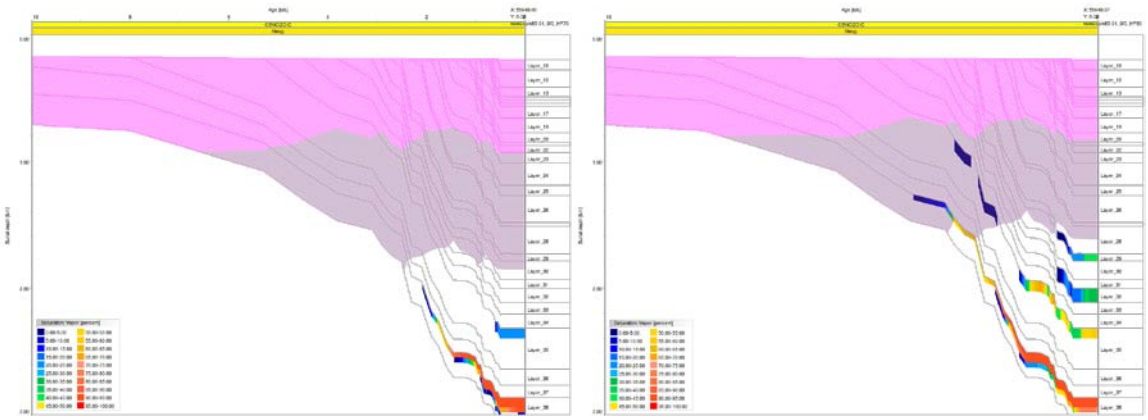

Figure 26. Hydrocarbon saturation over time in a pseudo well located 55.6 km from the south western end of line 85-01 (left: 70mW/m², right: 80mW/m²). To assess biodegradation temperature field is indicated by colour overlay as in Figure 23. Faults closed. Note: No accumulations were predicted for this location assuming a 60mW/m² scenario.

Predicted accumulations at 55.6km from the south western end of line 85-01 lie deep enough to have not been affected by biodegradation in the past and today.

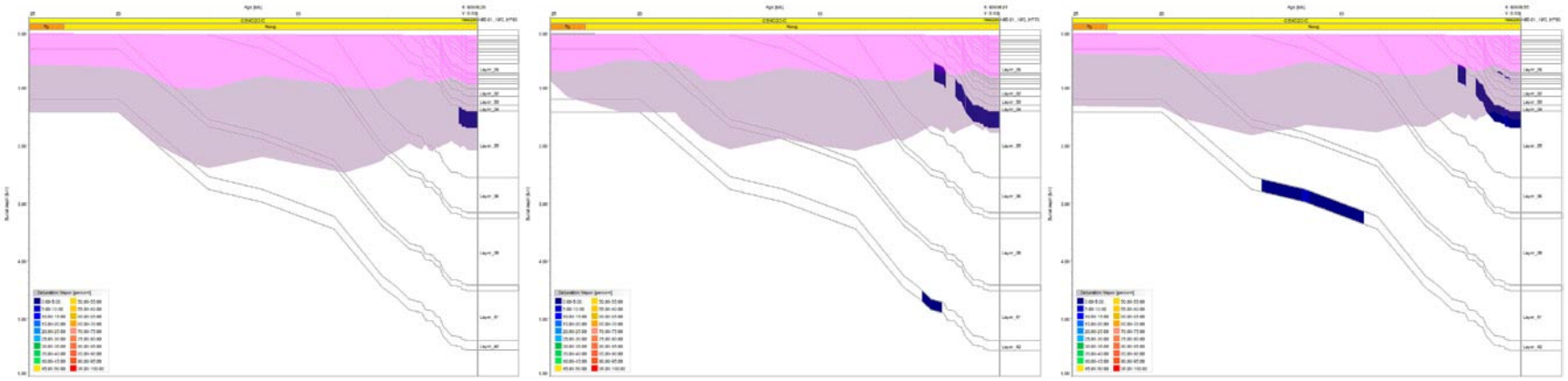

Figure 27. Hydrocarbon saturation over time in a pseudo well located 60.7 km from the south western end of line 85-01 (left: 60mW/m², middle: 70mW/m², right: 80mW/m²). To assess biodegradation temperature field is indicated by colour overlay as in Figure 23. Top row: Faults closed. Bottom row: Faults open. Note: Liquid instead of vapour saturation shown for 60mW/m scenario.

Very limited petroleum saturation is predicted for a location 60.7km from the south western end of line 85-01. If any accumulations were to have formed here, they might experience biodegradation today.

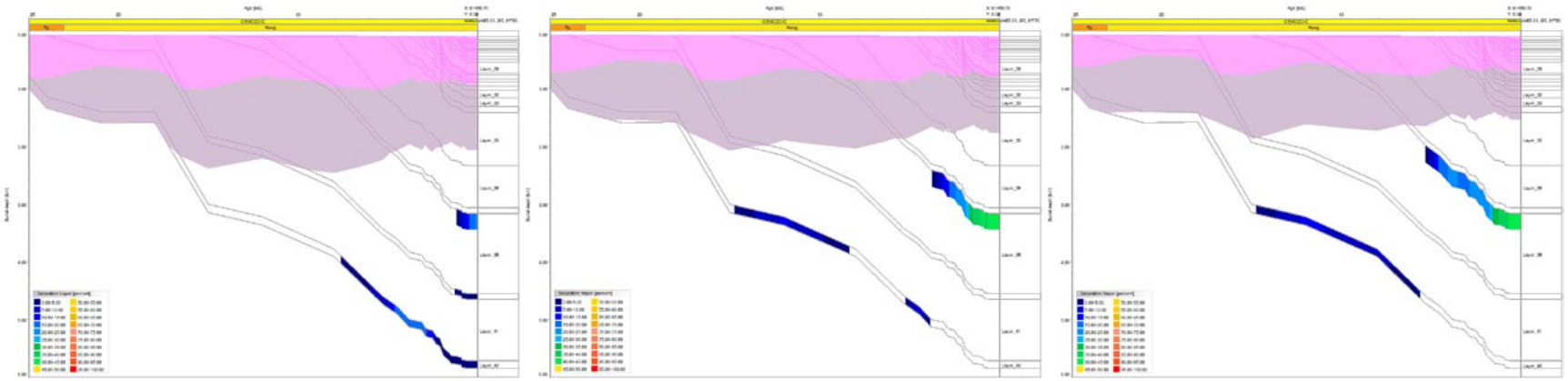

Figure 28. Hydrocarbon saturation over time in a pseudo well located 61.5 km from the south western end of line 85-01 (left: 60mW/m², middle: 70mW/m², right: 80mW/m²). To assess biodegradation temperature field is indicated by colour overlay as in Figure 23. Faults opened. Note: Liquid instead of vapour saturation shown for 60mW/m² scenario.

Predicted accumulations at 61.5km from the south western end of line 85-01 lie deep enough to have not been affected by biodegradation in the past and today.

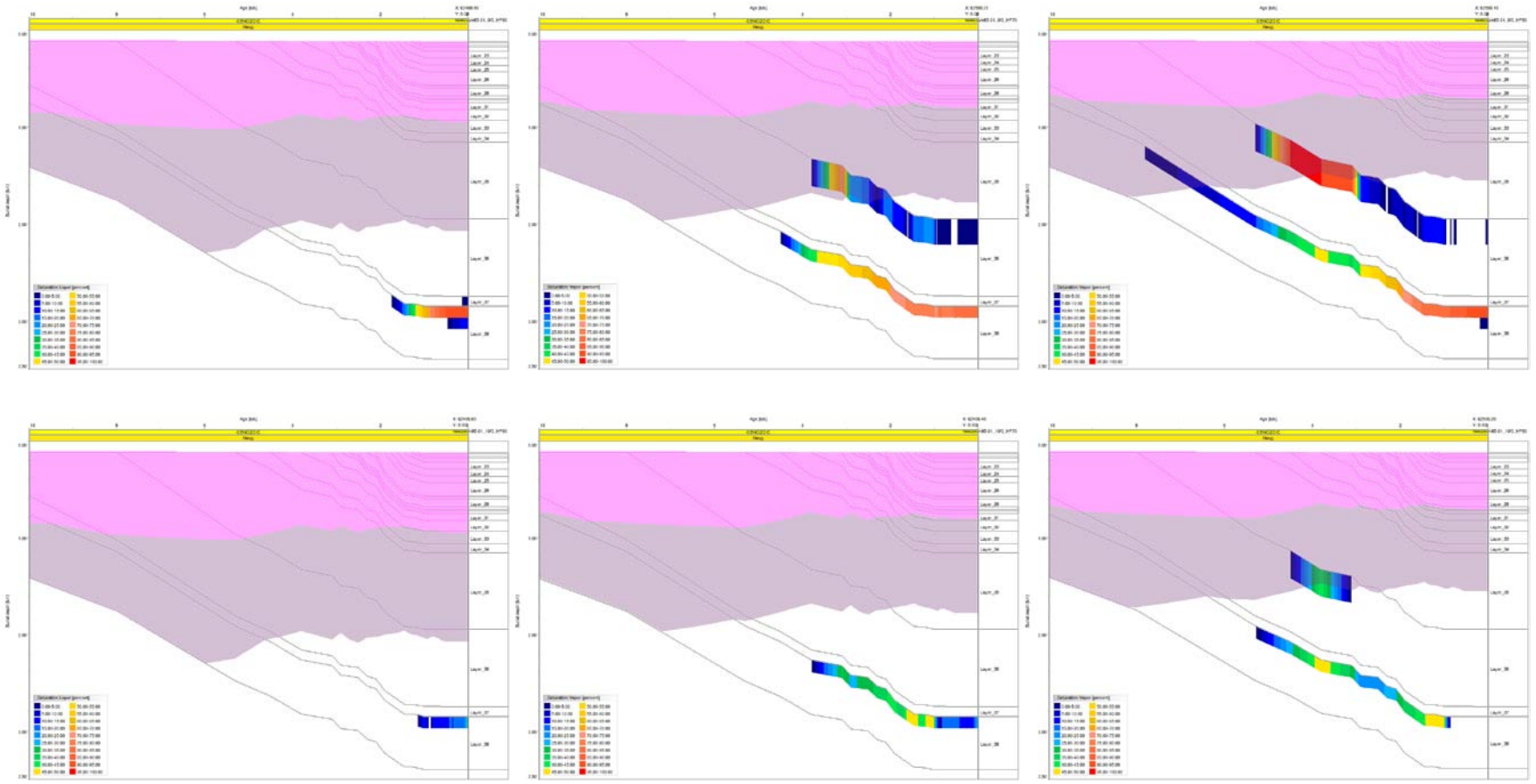

Figure 29. Hydrocarbon saturation over time in a pseudo well located 62.5 km from the south western end of line 85-01 (left: 60mW/m², middle: 70mW/m², right: 80mW/m²). To assess biodegradation temperature field is indicated by colour overlay as in Figure 23. Top row: Faults closed. Bottom row: Faults open. Note: Liquid instead of vapour saturation shown for 60mW/m² scenario.

Predicted accumulations at 62.5km from the south western end of line 85-01 lie deep enough today to not experience biodegradation, but the shallower ones might have been affected by biodegradation in the past.

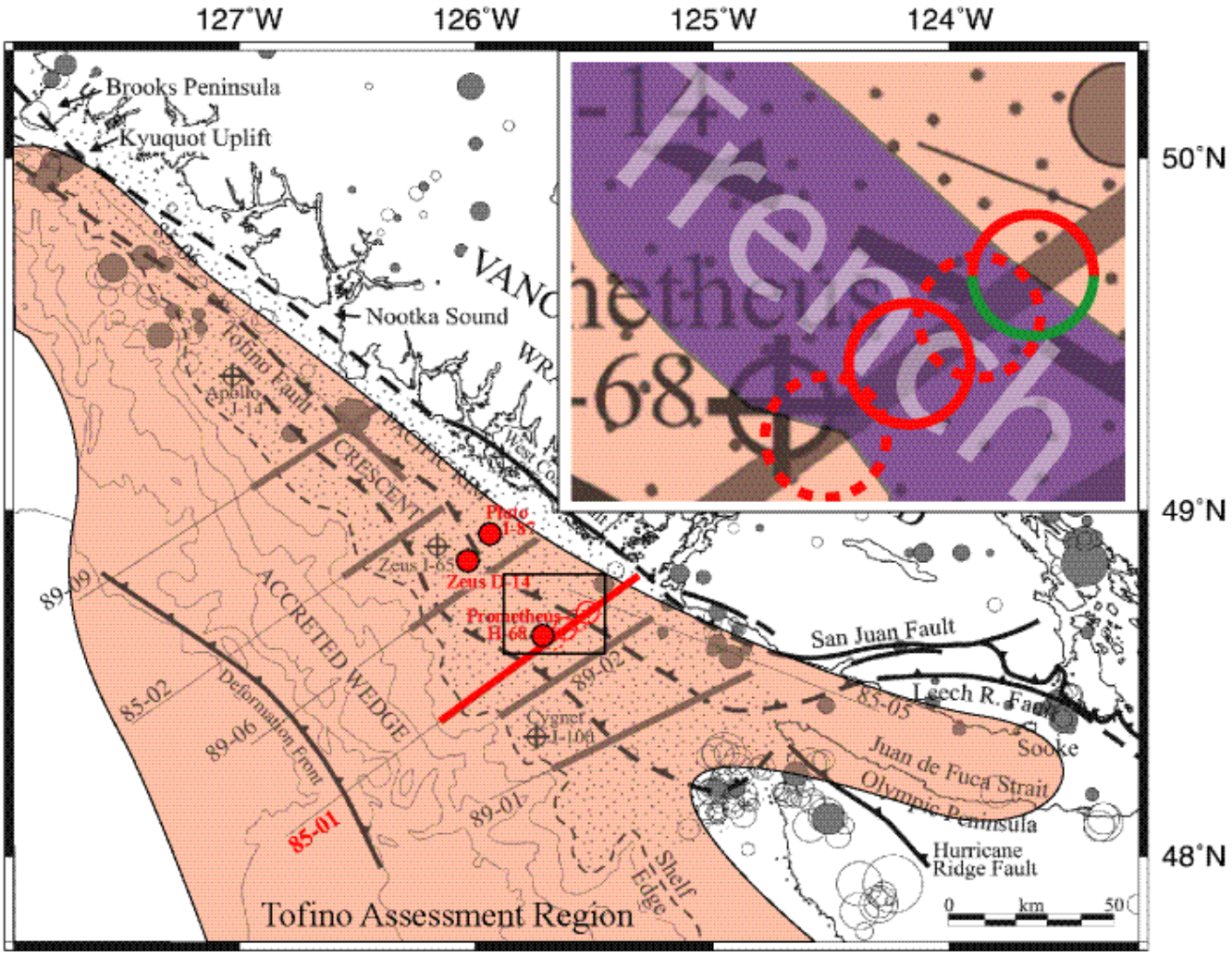

Figure 30. Bathymetry map of the Tofino Assessment Region with the sedimentary trench as interpreted based on gravity data from Dehler at al. (1992). As a first order approximation the extend of the hydrocarbon kitchen equals extend of the trench the but better mapping based on additional seismic reflection data is needed to more accurately outline its extend. Zones of predicted accumulations along the 2D transect presented in this study are shown in inset (green: oil, red: gas). Predicted accumulations in a central anticline structure and towards the southwest margin of the trench are often shallow and might be affected by recent biodegradation (dashed circles).

6 Discussion

6.1 Input parameters

Validity of predictions made using 2D basin modelling technology depends on quality of input. In the following the most sensitive parameters are presented and their influence on model predictions is discussed.

6.1.1 Lithology

Lateral homogeneity of lithology has been assumed along line 85-01. This approach was necessary due to sparse information concerning lateral variations. Such a large lateral extent of source, reservoir, and seal rocks may, however, draw an overly optimistic picture.

6.1.2 Presence of source rocks

Although the full extent of source rocks in the Tofino Basin is largely undetermined, TOC-enriched intervals extend uninterrupted over more than 10km in our models. Within the central trench or half-graben, timing of maturation may be unrealistically insensitive, because hydrocarbon would be generated and expelled over long periods of time due to varying burial.

Presence and nature of Mesozoic sequences below the Tofino Basin are unknown and the seismic data did not image this part of the section well. The Pacific Rim Complex exposed on Vancouver Island however forms a relatively small terrane consisting of two parts: the lower Ucluth Formation composed of lower Mesozoic arc-volcanics and the upper composed of Lower Cretaceous mélanges (Brandon, 1989). The latter comprises two units: Unit 1 - a Lower Cretaceous mudstone-rich mélange (up to 55% black mudstones) and Unit 2 - an overlying, undated sandstone-rich mélange. On the Ucluth Peninsula Unit 1 can be subdivided into two subunits exposed in opposite limbs of the Ucluth anticline. Despite the fact, that Cretaceous sourced petroleum systems are known to exist in the southern extension of the Tofino Basin in Washington and equivalent structures in Oregon we were not able to include them in our modelling due to lack of data. Hydrocarbon generation from Mesozoic source rocks may however prove to be a more promising exploration target in this region in the future.

6.1.3 Presence of reservoir rocks

Apart from the optimistic assumption of lateral homogeneity mentioned above, our modelling does not account for deterioration of arkosic reservoir strata due to diagenesis during burial. Such diagenesis could severely limit the quality of reservoir rocks below a certain depth.

6.2 Migration along faults

Flow along a given fault, at a given time is subject to many variables. In addition to tectonic influences, weathering of surrounding arkosic rocks may have plugged fault planes, causing limited permeability. Varying permeability along/across fault planes is

the most significant model variables affecting the number, size, and nature of accumulations. Neither of the scenarios models (faults completely open/ faults completely sealed) is realistic and they only serve as end members to a matrix of infinite possible models. They do however show the possible variability and the importance to address fault properties for future assessments of this region.

6.3 Calibration

Opportunities for calibration are sparse in Tofino Basin, which spans an area of approximately 25.000 km2 only drilled by six wells. Maturation profiles with depth at three proximal well locations show some variability (Figure 18). All wells however fall within the general maturation trend established for the area but only the Pluto I-87 drilled the deepest part of the central trench and shows reliable data with little scatter.

6.4 Risk factors

As discussed above, work in a frontier basin requires a fair amount of inference based on limited data available. Consequently, a number of variables used in the model presented here are unknown or projected from a sparse dataset into a large frontier basin favouring preservation of hydrocarbons; we summarize them below:

- **Existence and character of source rocks**. Our assumption of wide distribution of source rocks, both in depth and lateral, might be an optimistic one and ensures that hydrocarbons were generated over long periods of time (tens of millions of years) and have a greater likelihood of being trapped.
- **Effectiveness of seals**. No data is available to assess the sealing qualities of the cap rocks in our models and our assumptions might paint an overoptimistic picture.
- **Biodegradation** presents a significant risk for Tertiary traps because some are predicted to lie at depths of less than 1800 m and in temperatures of 80^{o}C or less. The current high rate of generation, however, may result in gas being fed from below replacing, that which has been degraded. Most of the Mesozoic sourced traps lie below the zone of possible biodegradation.

6.5 Outlook

Many of the risk factors we have raised can not be realistically assessed without better structural information from high-frequency 3D datasets and better lithologic information from wells. This work can not be done under the current moratorium on exploration in this basin. However, some work could usefully be done using existing data and samples. Newly develloped, less intrusive methods of investigation might also be used under the current moratorium. Some examples below:

- **Apatite fission track analyses (AFTA)** could be used on available well samples to determine burial and thermal history of sediments at well locations.
- **Multi-component kerogen kinetics** could be established for available source rock samples which in turn would allow for much refined PSMs.
- **Better understanding of the underlying Mesozoic rocks** would enable to incorporate a Mesozoic sourced petroleum system into the PSM

7 References

Brandon, M.T. (1989). Deformation styles in a sequence of olistostromal mélanges, Pacific Rim Complex, western Vancouver Island, Canada. *Geol. Soc. Am. Bull.*, v. 101, p. 1520-1542.

Burnham A.K., (1989). A simple kinetic model of petroleum formation and cracking. Report UCID-21665, Lawrence Livermore National Laboratory.

Burnham, A.K. and Sweeney, J.J. (1989). A chemical model of vitrinite maturation and reflectance. *Geochimica et Cosmochimica Acta*, v. 53, p. 2649-2657.

Bustin, R.M. (1995). Organic maturation and petroleum source rock potential of Tofino Basin, southwestern British Columbia. *Bulletin of Canadian Petroleum Geology*, v. 43(2), p. 177-186.

Davis, E.E., Hyndman, R.D., and Villinger, H. (1990). Rates of fluid expulsion across the northern Cascadia accretionary prism: constraints from new heat flow and multichannel seismic reflection data. *Journal of Geophysical Research*, v. 95, p. 8.860-8.889.

Dehler, S.A. and Clowes, R.M. (1992). Integrated geophysical modelling of terranes and other structural features along the western Canadian margin. Can. J. Earth Sci., v. 29, 1492-1508.

Dewing, K. and Sanei, H. (2008). Analysis of large thermal maturity datasets: Examples fromthe Canadian Arctic Islands. International Journal of Coal Geology,v. 77, p.436-448

Espitalie, J., Deroo, G., Marquis, F. (1985). Rock Eval pyrolysis and its applications. Preprint; Institut Francais du Petrole, Geologie No. 27299, 72 p. English translation of: La pyrolyse Rock-Eval et ses applications, Premiere, Deuxieme et Troisieme Parties. Revue de l'Institut Francais du Petrole 40, 563–579 and 755–784; 41, 73–89.

Ganguly, N., Spence, G.D., Chapman, N.R., and Hyndman, R.D. (2000). Heat flow variations from bottom simulating reflectors on the Cascadia margin. *Marine Geol*ogy, v. 164, p. 53-68.

Hannigan, P. K., Dietrich, J.R., Lee, P.J. and Osadetz, K.G. (2001). Petroleum Resource Potential of Sedimentary Basins on the Pacific Margin of Canada. *Geological Survey of Canada Bulletin*, v. 564, 74 pp.

Hayward, N. and Calvert, A.J. (2007). Seismic reflection and tomographic velocity model constraints on the evolution of the Tofino forearc basin, British Columbia. *Geophys. J. Int.* (2007) 168, 634–646.

He, J.; Wang, K.; Dragert, H.; Miller, M.M. (2003). Spherical viscoelastic finite element model for Cascadia interseismic deformation. Eos, Transactions, American Geophysical Union, vol.84, no.46, Suppl., pp.1090.

Hyndman, R.D.; Yorath, C.J.; Clowes, R.M.; Davis, E.E. (1990). The northern Cascadia subduction zone at Vancouver Island; seismic structure and tectonic history Canadian Journal of Earth Sciences = Revue Canadienne des Sciences de la Terre, vol. 27, no. 3, pp.313-329.

Hyndman, R.D., Foucher, J.P., Yamano, M., and Fisher, A. (1992): Deep sea bottom-simulating-reflectors: calibration of the base of the hydrate stability field as used for heat flow estimates. *Earth and Planetary Science Letters*, v. 109, p. 289-301.

Hyndman, R. D., and Hamilton, T. S. (1993). Queen Charlotte area Cenozoic tectonics and volcanism and their Association with relative plate motions along the northeastern Pacific margin. *Journal of Geophysical Research*, v. 98, p. 14.257-14.277.

Hyndman, R.D., Spence, G.D., Yuan, T., and Davis, E.E. (1994). Regional geophysics and structural framework of the Vancouver Island margin accretionary prism. *Proceedings of the Ocean Drilling Program, Initial Reports*, v. 146(1), p. 399-419.

Hyndman, R.D. and Wang, K. (1993). Thermal constraints on the zone of major thrust earthquake failure: the Cascadia subduction zone, J. Geophys. Res. 98 (1993), pp. 2039-2060.

Johns, M.J., Barnes, C.R., and Narayan, Y.R. (2006). Cenozoic ichthyolith biostratigraphy: Tofino Basin, British Columbia. *Can. J. Earth Sci.*, v.43, p. 177-204.

Kvenvolden, K.A; Barnard, L.A. (1983). Gas hydrates of the Blake Outer Ridge, Site 533, Deep Sea Drilling Project Leg 76. Initial Reports of the Deep Sea Drilling Project, vol. 76, pp.353-365.

Langseth, M.G. and Hobart, M.A. (1984). A marine geothermal study over deformed sediments of the subduction complex off Oregon and Washington Eos, Transactions, American Geophysical Union, vol.65, no.45, pp.1089

Lewis, T.J.; Bentkowski, W.H.; Davis, E.E.; Hyndman, R.D.; Souther, J.G.; and Wright, J.A. (1988). Subduction of the Juan de Fuca Plate; thermal consequences. Journal of Geophysical Research, vol. 93, no. B12, pp.15,207-15,225.

Lewis, T.J., Bentowski, W.H., and Wright, J.A. (1991a). Thermal state of the Queen Charlotte Basin, British Columbia: warm. In Evolution and Hydrocarbon Potential of the Queen Charlotte Basin, British Columbia, Geological Survey of Canada, Paper 90-10, p. 489-506.

Monger, J.W.H.; Price, R.A.; and Tempelman-Kluit, D.J. (1982). Tectonic accretion and the origin of the two major metamorphic and plutonic welts in the Canadian Cordillera Geology (Boulder), vol.10, no.2, pp.70-75.

Narayan, Y.R. (2003). A new Cenozoic foraminiferal biostratigraphy, paleoecology (biofacies) and strontium isotope study of Shell Canada exploration wells from the Tofino Basin, offshore Vancouver Island, British Columbia. Thesis; Doctoral, University of Victoria, Victoria, BC, Canada.

Narayan, Y.R.; Barnes, C.R.; Johns, M.J. (2005). Taxonomy and biostratigraphy of Cenozoic foraminifers from Shell Canada wells, Tofino Basin, offshore Vancouver Island, British Columbia. Micropaleontology, vol.51, no.2, pp.101-168.

Parsons and Sclater (1977). An analysis of the variation of ocean floor bathymetry and heat flow with age. Journal of Geophysical Research, vol. 82, no. 5, pp.803-827.

Pohlman, J.W., Canuel, E.A., Chapman, N.R., Spence, G.D., Whiticar, M.J., and Coffin, R.B. (2005). The origin of thermogenic gas hydrates on the northern Cascadia Margin as inferred from isotopic ($^{13}C/^{12}C$ and D/H) and molecular composition of hydrate and vent gas. *Organic Geochemistry*, v. 36, p. 703-716.

Riedel, M. (2001). 3-D seismic investigations of northern Cascadia marine gas hydrates. Thesis; Doctoral, University of Victoria, Victoria, BC, Canada.

Riedel, M., Willoughby, E.C., Chen, M.A., He, T., Novosel, I., Schwalenberg, K., Hyndman, R.D., Spence, G.D., Chapman, N.R., and Edwards, R.N. (2006). Gas hydrate on the northern Cascadia margin: regional geophysics and structural framework. *Proceedings of the Integrated Ocean Drilling Program,* v. 311.

Sassen, R.; MacDonald, I.R. (1994). Evidence of structure H hydrate, Gulf of Mexico continental slope. Organic Geochemistry, vol.22, no.6, pp.1029-1032.

Shipley, T.H.; Houston, M.H.; Buffler, R.T.; Shaub, F.J.; McMillen, K.J.; Ladd, J.W.; Worzel, J.L. (1979). Seismic evidence for widespread possible gas hydrate horizons on continental slopes and rises AAPG Bulletin, vol.63, no.12, pp.2204-2213.

Shouldice, D.H. (1971). Geology of the western Canadian continental shelf. Bull. Can. Pet. Geol., v. 19(2), p.405-436.

Shouldice, D.H. (1973). Geology of Western Canadian Continental Shelf. The American Association of Petroleum Geologists Bulletin, vol.56, no.9, pp.1908-1909.

Spence, G. D.; Hyndman, R.D.; Chapman, N.R.; Walia, R.; Gettrust, J.; Edwards, R.Nl. (1991). North Cascadia deep sea gas hydrates. Annals of the New York Academy of Sciences, vol.912, pp.65-75

Spence, G.D.; Hyndman, R.D.; Chapman, N.R.; Riedel, M.; Edwards, N.; and Yuan, J. (2000). Cascadia margin, Northeast Pacific Ocean; hydrate distribution from geophysical investigations Coastal Systems and Continental Margins, vol. 5, pp.183-198.

Wang, K.; Dragert, H.; Melosh, H.J. (1994). Finite element study of uplift and strain across Vancouver Island. Canadian Journal of Earth Sciences = Revue Canadienne des Sciences de la Terre, vol. 31, no. 10, pp.1510-1522.

Wang, K., Mulder, T., Rogers, G.C., and Hyndman, R.D. (1995). Case for very low coupling stress on the Cascadia subduction fault. J.Geoph.Res., v. 100, p. 12.907-12.918.

Yorath, C.J.; Hyndman, R.D.; Clowes, R.M. (1987). Structure and accretion style of the modern convergent margin of Western Canada. Program with Abstracts - Geological Association of Canada; Mineralogical Association of Canada: Joint Annual Meeting, vol. 12, pp.102.

8 Appendix

8.1 Predicted present day vitrinite reflectance

8.1.1 Constant heat flow of 60 mW/m²

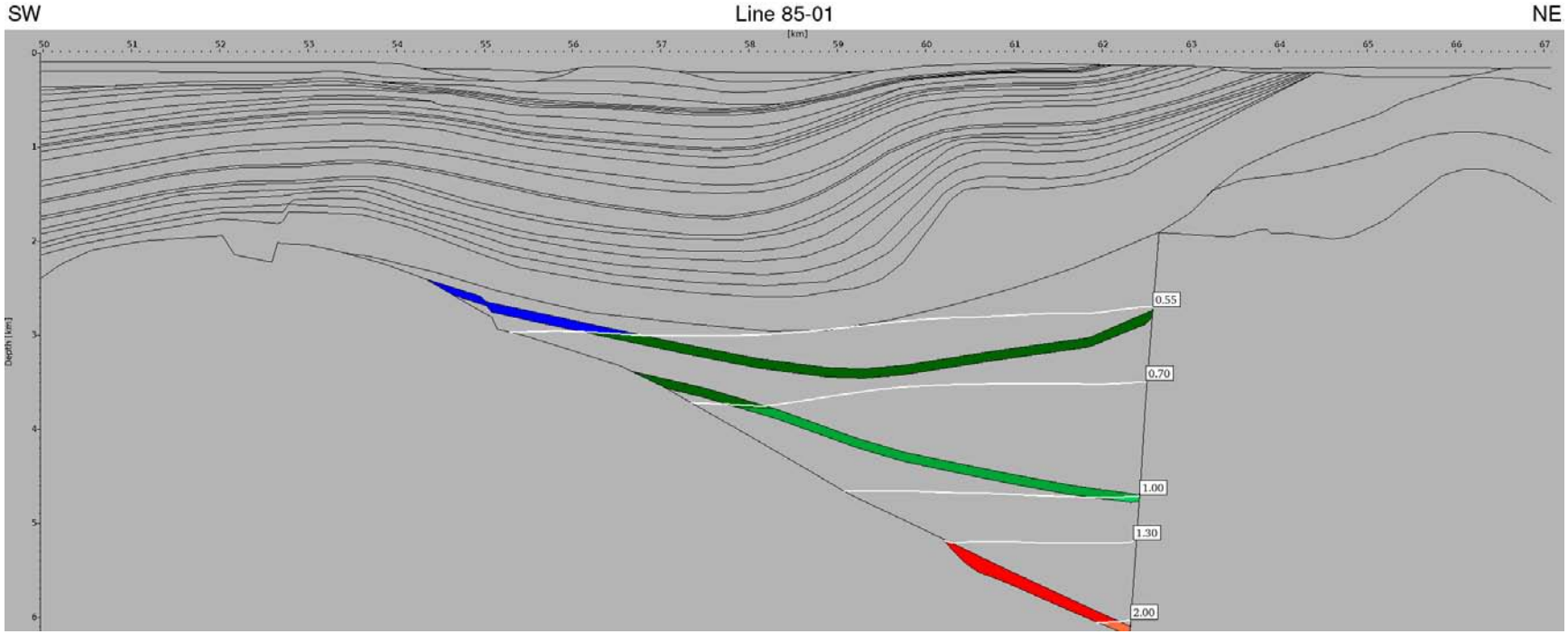

Figure 31 Predicted present day vitrinite reflectance along line 85-01, assuming a lateral and time constant heat flow of 60 mW/m².

8.1.2 Constant heat flow of 70 mW/m²

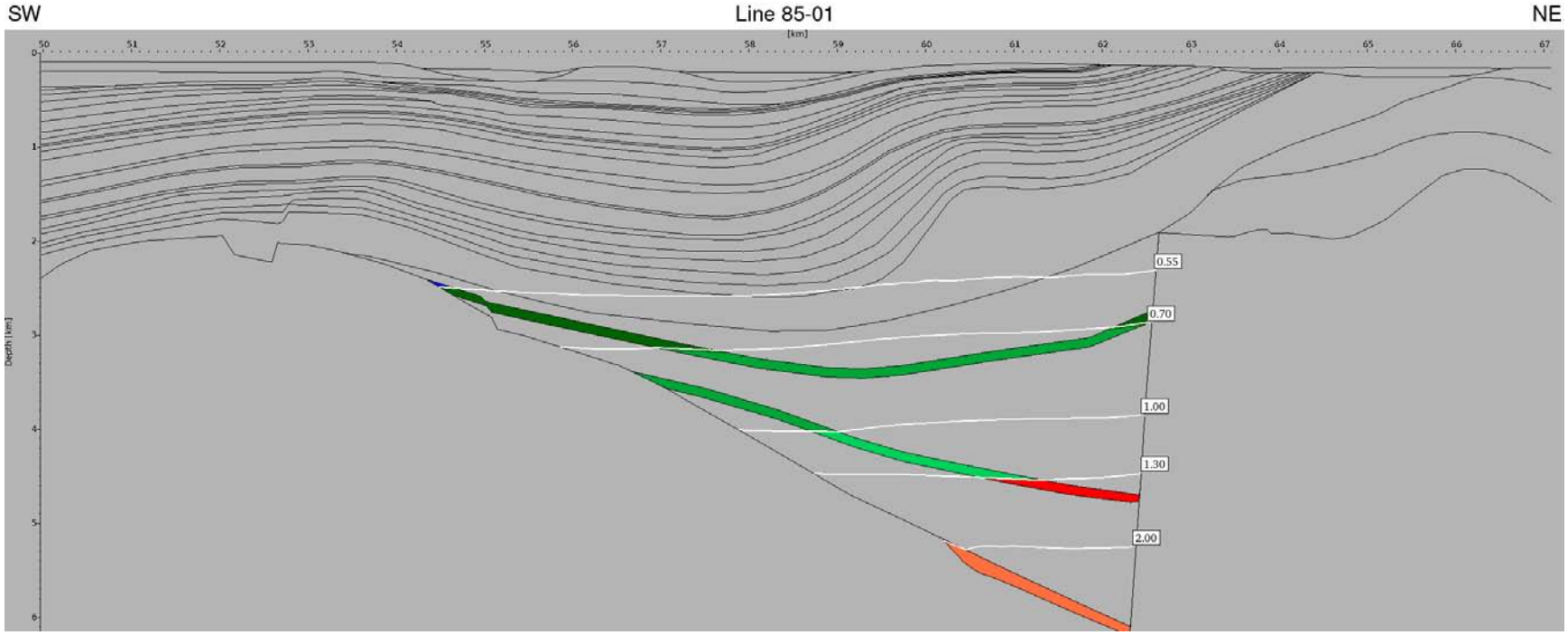

Figure 32 Predicted present day vitrinite reflectance along line 85-01, assuming a lateral and time constant heat flow of 70 mW/m².

8.1.3 Constant heat flow of 80 mW/m²

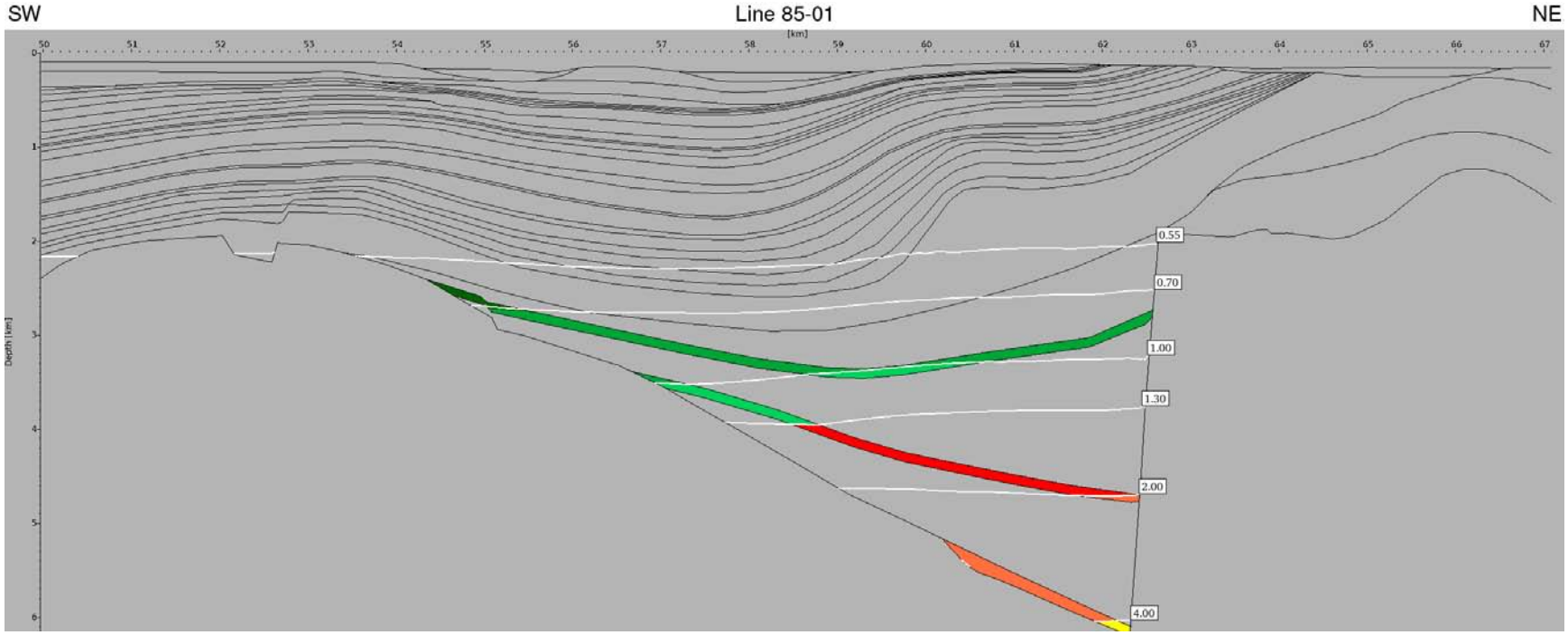

Figure 33 Predicted present day vitrinite reflectance along line 85-01, assuming a lateral and time constant heat flow of 80 mW/m².

8.2 Predicted accumulations

8.2.1 Constant heat flow of 60 mW/m²

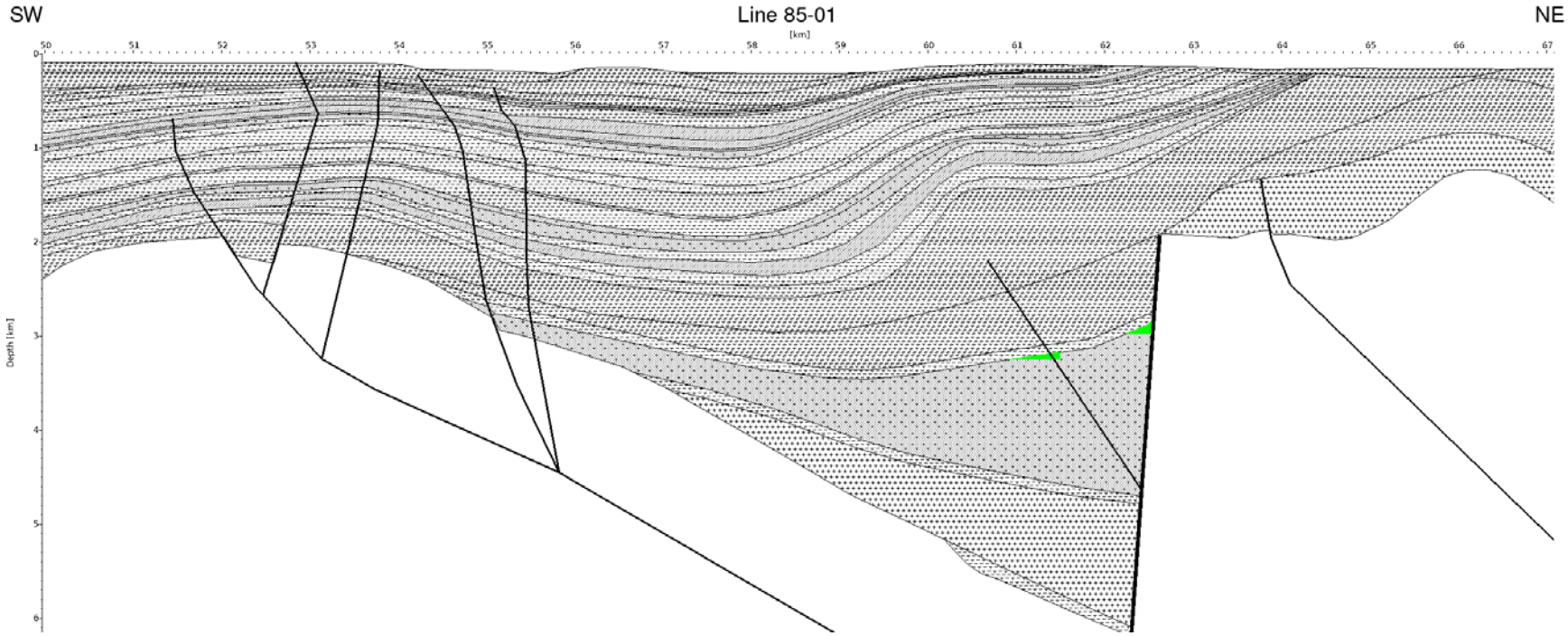

Figure 34 Predicted accumulations along line 85-01, assuming a no enhanced fault permeability and a constant heat flow of 60 mW/m². For legend see Figure 32.

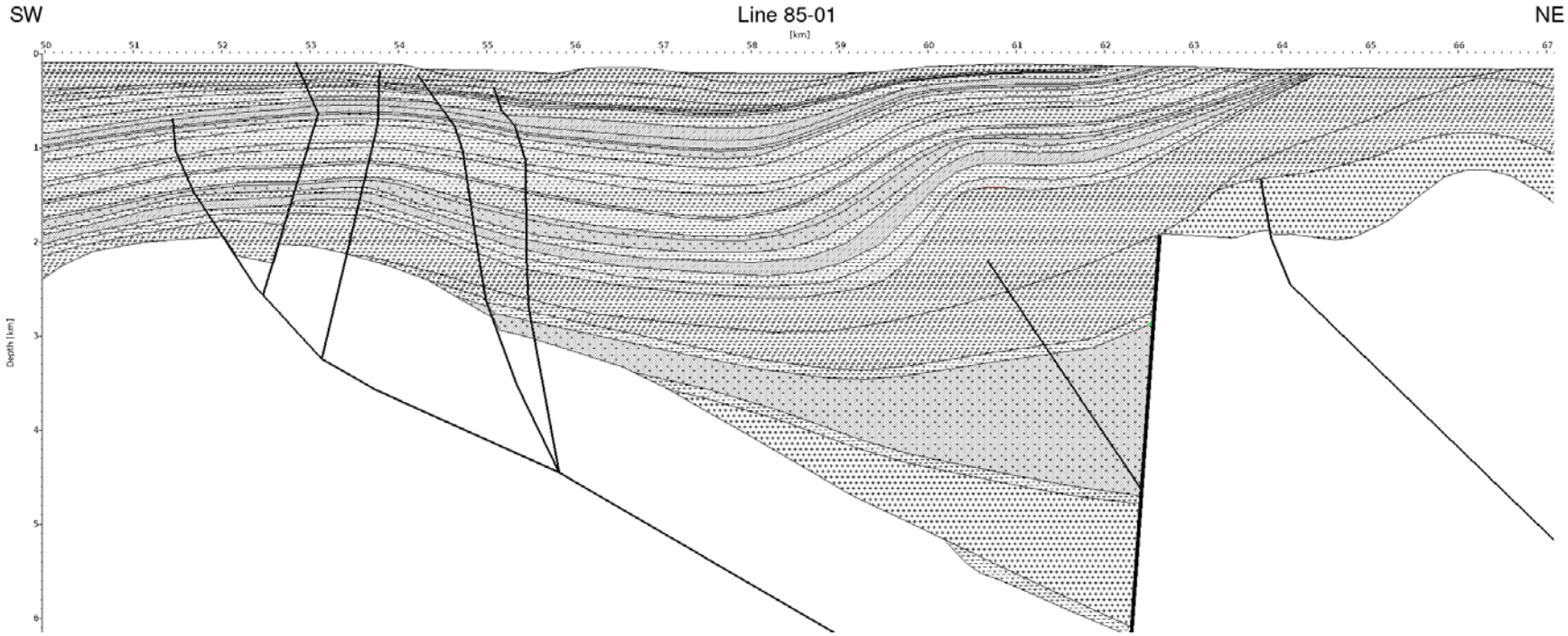

Figure 35 Predicted accumulations along line 85-01, assuming enhanced fault permeability and a constant heat flow of 60 mW/m². For legend see Figure 32.

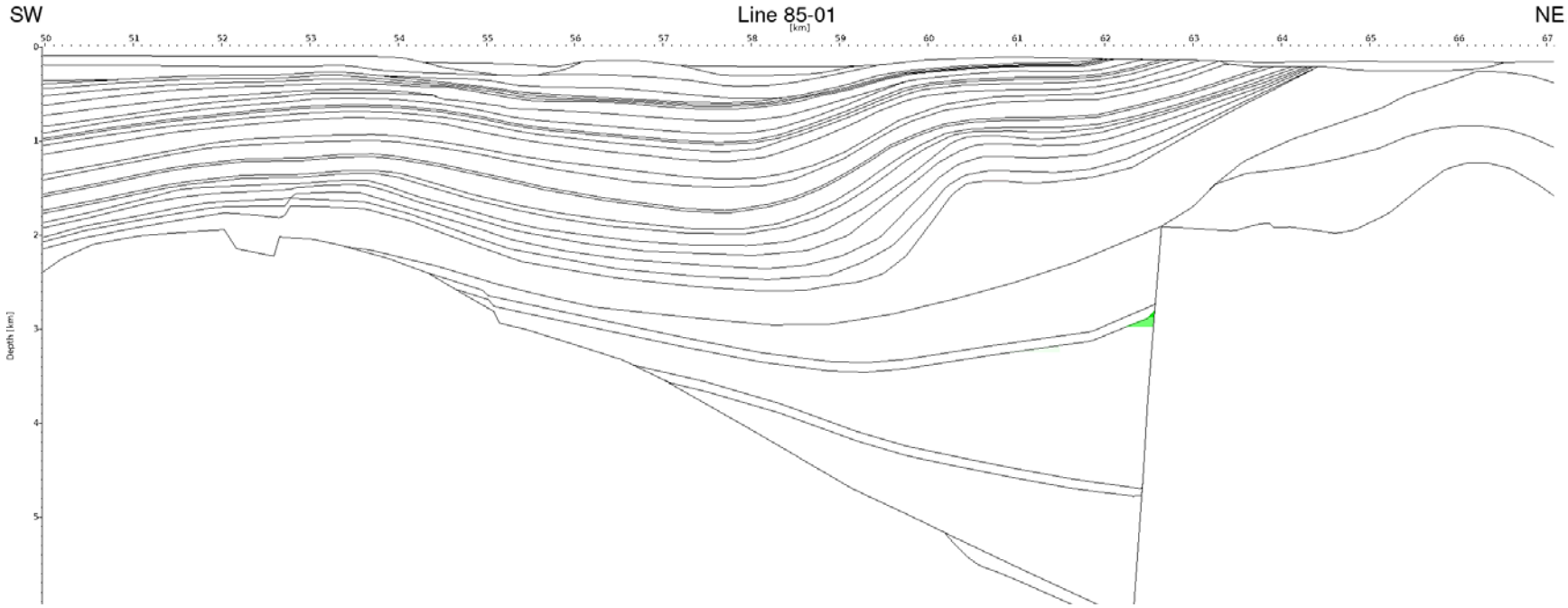

Figure 36 Predicted accumulations along line 85-01 averaged over both scenarios, assuming a constant heat flow of 60 mW/m². Intensity of colour reflects number of scenarios that each accumulation occurs in. For legend see Figure 32.

8.2.2 Constant heat flow of 70 mW/m²

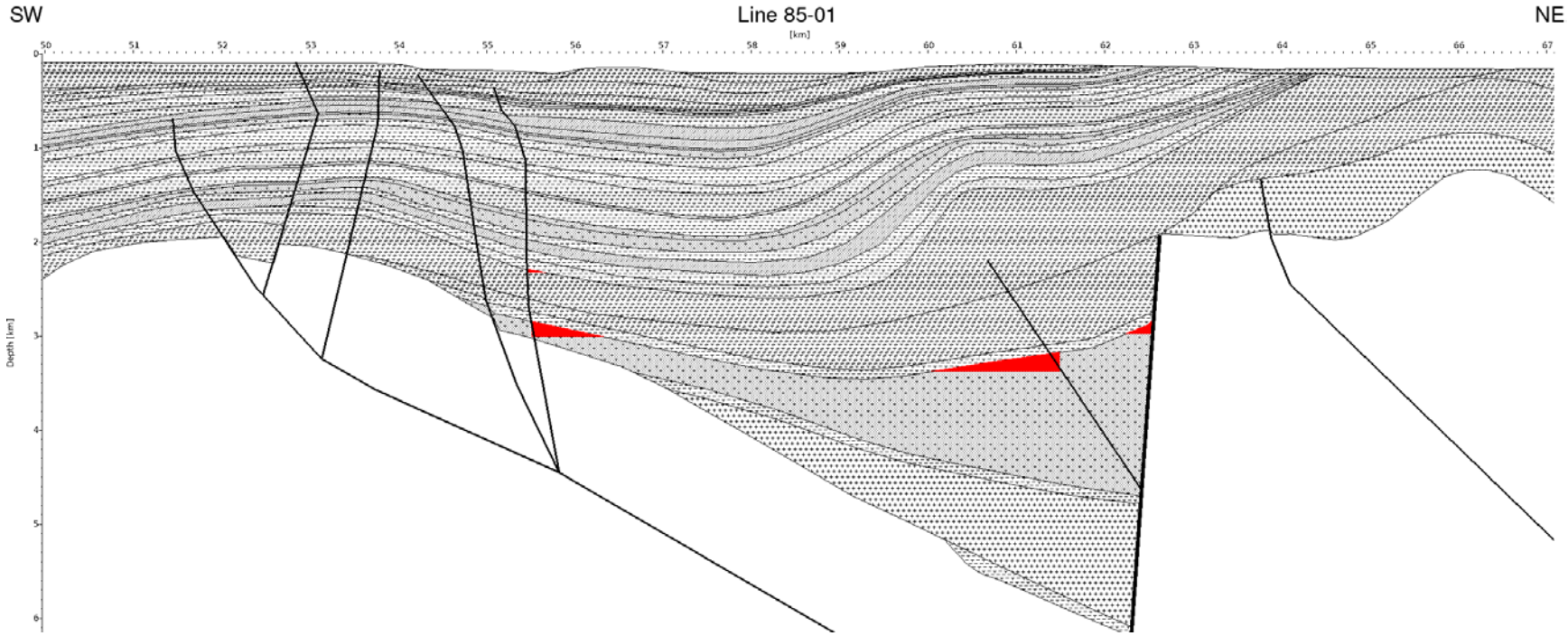

Figure 37 Predicted accumulations along line 85-01, assuming a no enhanced fault permeability and a constant heat flow of 70 mW/m². For legend see Figure 32.

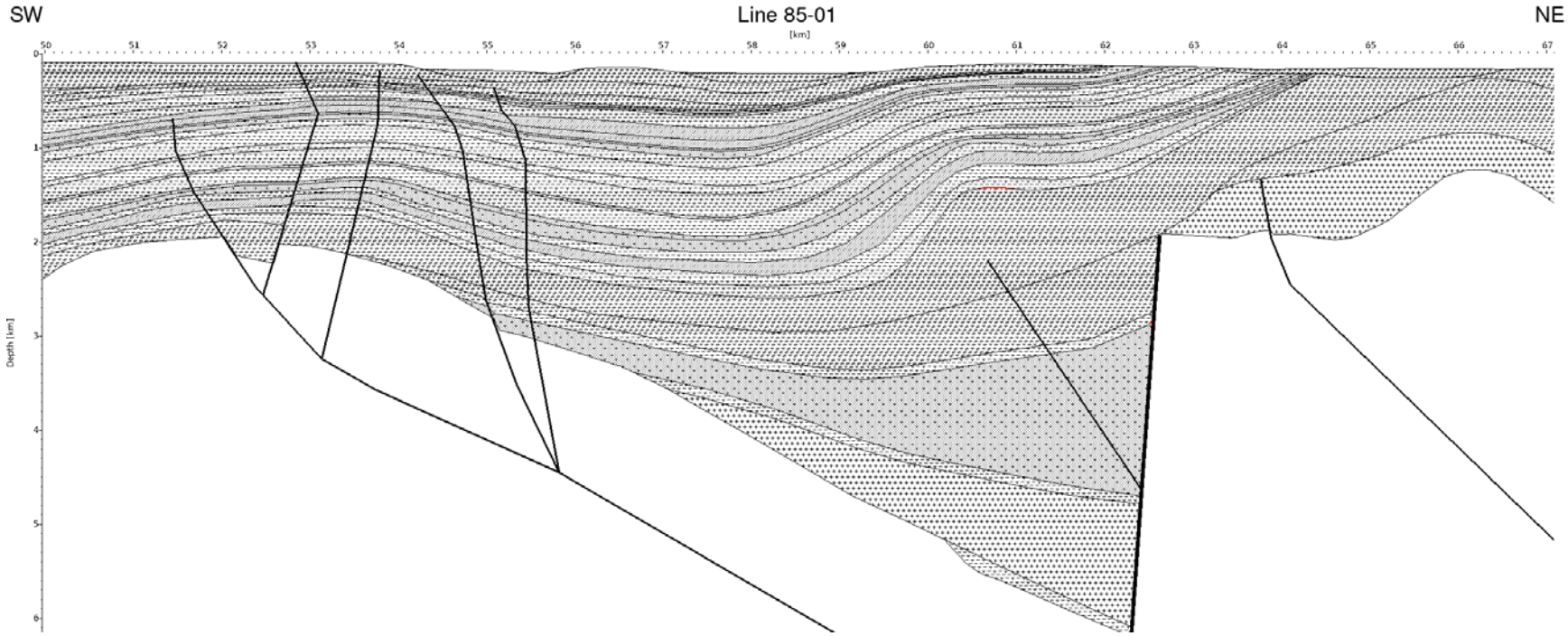

Figure 38 Predicted accumulations along line 85-01, assuming enhanced fault permeability and a constant heat flow of 70 mW/m². For legend see Figure 32.

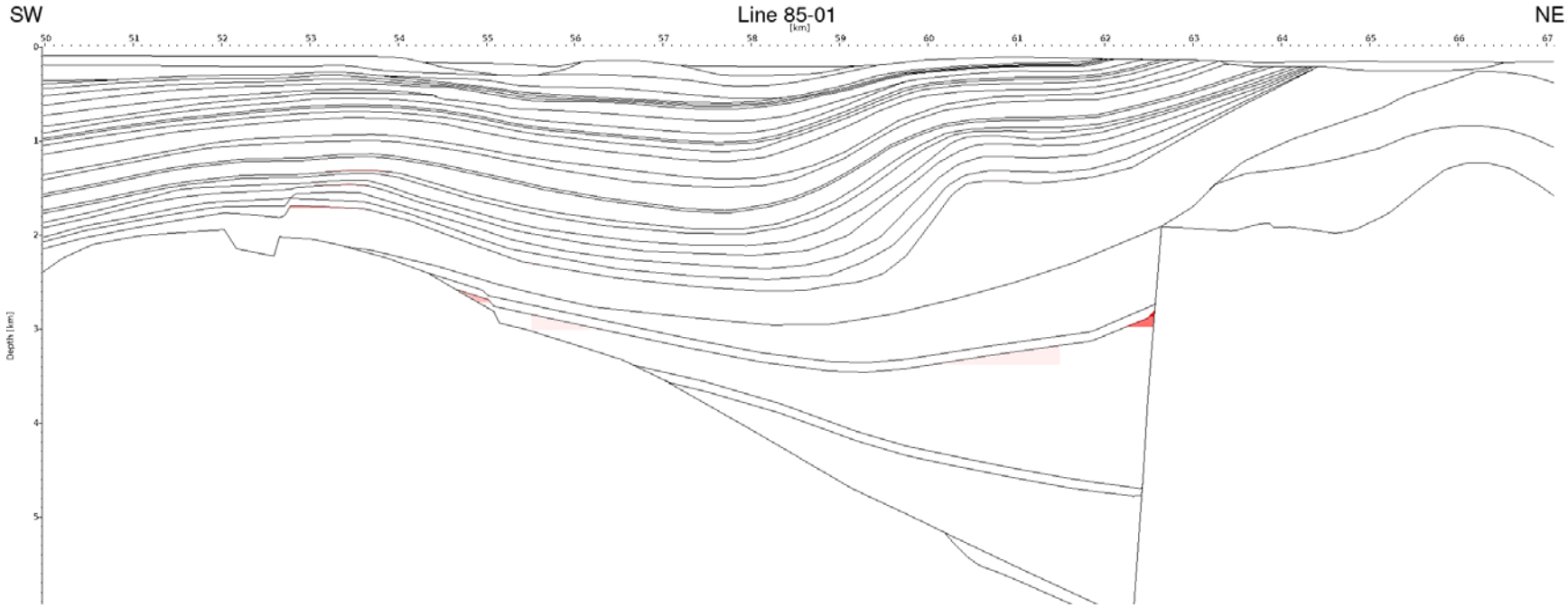

Figure 39 Predicted accumulations along line 85-01 averaged over both scenarios, assuming a constant heat flow of 70 mW/m². Intensity of colour reflects number of scenarios that each accumulation occurs in. For legend see Figure 32.

8.2.3 Constant heat flow of 80 mW/m²

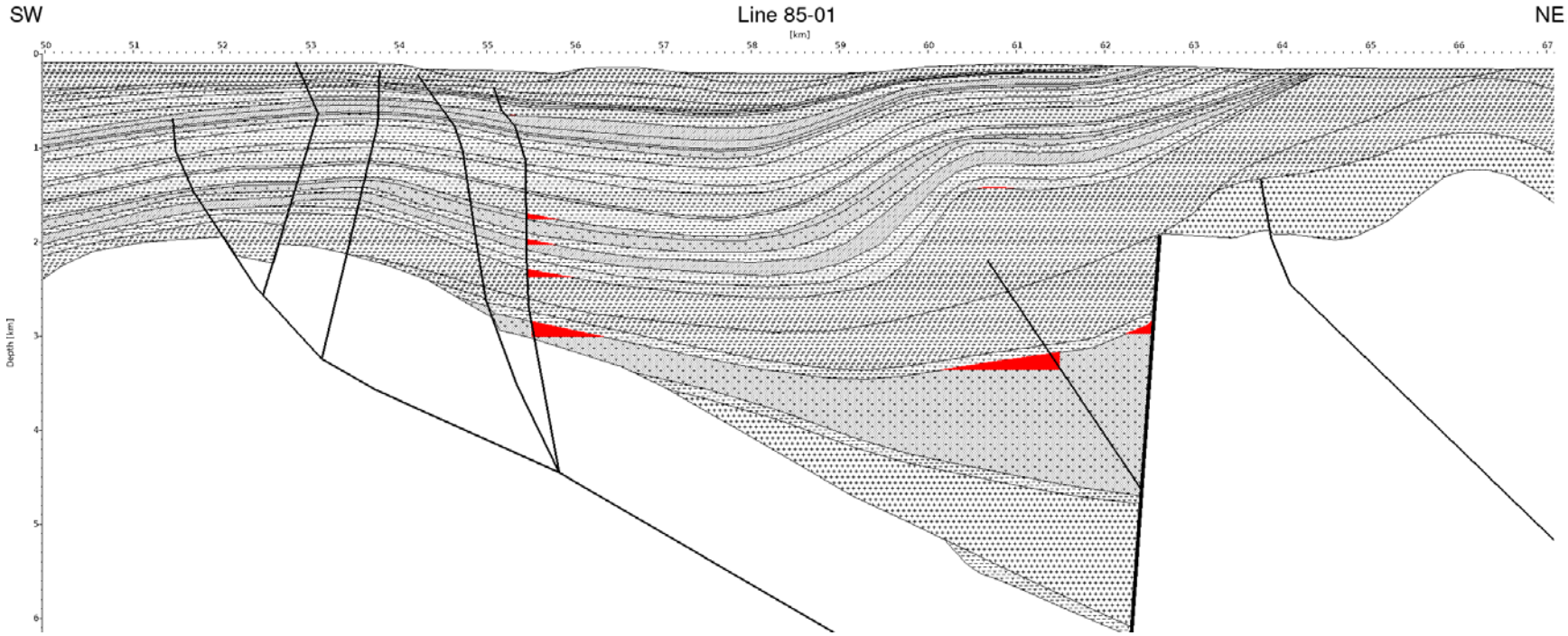

Figure 40 Predicted accumulations along line 85-01, assuming a no enhanced fault permeability and a constant heat flow of 80 mW/m². For legend see Figure 32.

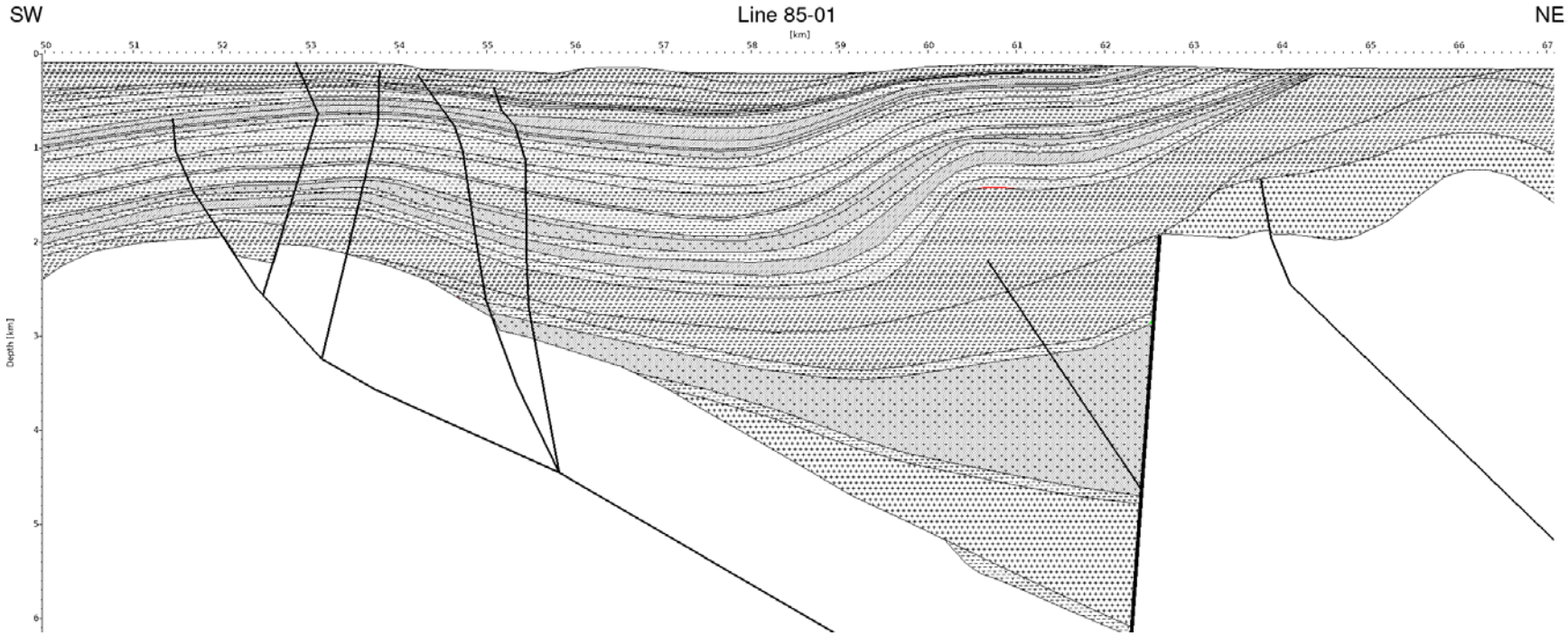

Figure 41 Predicted accumulations along line 85-01, assuming enhanced fault permeability and a constant heat flow of 80 mW/m². For legend see Figure 32.

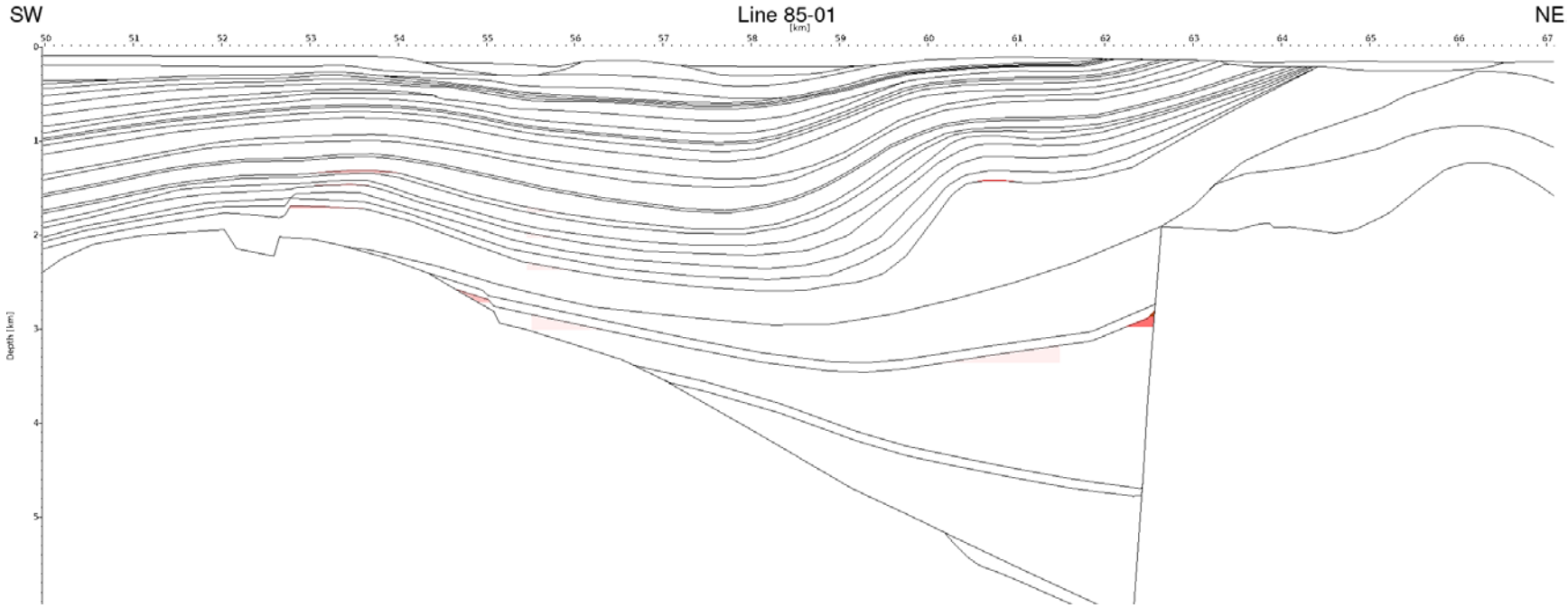

Figure 42 Predicted accumulations along line 85-01 averaged over both scenarios, assuming a constant heat flow of 80 mW/m². Intensity of colour reflects number of scenarios that each accumulation occurs in. For legend see Figure 32.